

PRESENTATIONS AND
PUBLICATIONS

LIST OF CONFERENCES PRESENTATIONS

1. **Hiral Patel**, Kranti Bhamnote, Devarshi Gajjar (2022) Persister cell formation in clinical isolates of *Pseudomonas aeruginosa*. A poster presented at “The 2nd International Electronic Conference on Antibiotics—Drugs for Superbugs: Antibiotic Discovery, Modes of Action And Mechanisms of Resistance (ECA2022)” held virtually from 15 to 30 June 2022.
2. **Hiral Patel**, Devarshi Gajjar (2020) *Pseudomonas aeruginosa* Biofilms: Difference in strong and weak biofilms. Poster presented at “BioSangam 2020 — International Conference on Biotechnological Interventions for Societal Development” held at Department of Biotechnology, Motilal Nehru National Institute of Technology (MNNIT) Allahabad from 21 to 23 February 2020

LIST OF AWARDS

1. **CSIR-JRF fellowship** by CSIR-UGC, Government of India to carry out the Ph.D. work. November 2017 to November 2022

LIST OF PUBLICATIONS

1. Patel, Hiral, Hasmatbanu Buchad, and Devarshi Gajjar. "*Pseudomonas aeruginosa* persister cell formation upon antibiotic exposure in planktonic and biofilm state." *Scientific reports* 12, no. 1 (2022): 1-12.
2. Patel, Hiral, and Devarshi Gajjar. "Cell adhesion and twitching motility influence strong biofilm formation in *Pseudomonas aeruginosa*." *Biofouling* 38, no. 3 (2022): 235-249.



Biofouling
The Journal of Bioadhesion and Biofilm Research

Biofouling

The Journal of Bioadhesion and Biofilm Research

ISSN: (Print) (Online) Journal homepage: <https://www.tandfonline.com/loi/gbif20>



Cell adhesion and twitching motility influence strong biofilm formation in *Pseudomonas aeruginosa*

Hiral Patel & Devarshi Gajjar

To cite this article: Hiral Patel & Devarshi Gajjar (2022) Cell adhesion and twitching motility influence strong biofilm formation in *Pseudomonas aeruginosa*, *Biofouling*, 38:3, 235-249, DOI: 10.1080/08927014.2022.2054703

To link to this article: <https://doi.org/10.1080/08927014.2022.2054703>

 [View supplementary material](#) 

 Published online: 28 Mar 2022.

 [Submit your article to this journal](#) 

 Article views: 240

 [View related articles](#) 

 [View Crossmark data](#) 

Full Terms & Conditions of access and use can be found at
<https://www.tandfonline.com/action/journalInformation?journalCode=gbif20>



Cell adhesion and twitching motility influence strong biofilm formation in *Pseudomonas aeruginosa*

Hiral Patel and Devarshi Gajjar 

Department of Microbiology and Biotechnology Centre, Faculty of Science, The Maharaja Sayajirao University of Baroda, Vadodra, Gujarat, India

ABSTRACT

In the present study, biofilm formation was quantified in UTI isolates of *Pseudomonas aeruginosa* ($n=22$) using the crystal violet assay and was categorized into; strong ($n=16$), weak ($n=4$), and moderate ($n=2$) biofilm producers. Further experiments were done using strong ($n=4$) and weak ($n=4$) biofilm producers. Biofilm formation was greater in Luria broth followed by natural urine and artificial urine on silicone and silicone-coated latex. Cell adhesion and twitching motility were greater in strong biofilm producers. The presence of thick biofilm with an increased number of dead and total number of cells of strong biofilm producers was observed using CLSM. The concentrations of exopolymeric substances (eDNA, protein, and pel polysaccharide) were high in strong biofilm producers. FEG-SEM visualization of biofilm produced by strong biofilm producers showed more cells encased in thick biofilm matrix than weak ones. Overall results provide evidence for increased cell adhesion and twitching motility in strong biofilm producers.

ARTICLE HISTORY

Received 3 September 2021
Accepted 14 March 2022

KEYWORDS

Biofilm; UTI; strong; twitching motility

Introduction

Pseudomonas aeruginosa is an opportunistic pathogen responsible for causing infections like cystic fibrosis, endocarditis, pneumonia, bacteremia, and Urinary Tract Infections (UTIs) (Shigemura et al. 2006; Gomila et al. 2018). Catheter-Associated Urinary Tract Infections (CAUTIs) contribute significantly to hospital-associated infections (HAIs) (Lara-Isla et al. 2017), which are often persistent due to infections caused by biofilm-forming bacteria. *P. aeruginosa* is the third most common pathogen associated with hospital-acquired CAUTIs (Jarvis and Martone 1992; Djordjevic et al. 2013). In a study from India, *P. aeruginosa* accounted for 15% of all bacterial isolates collected from a tertiary care hospital over a period of 2012 to 2016 (Kumari et al. 2019). Infections caused by *P. aeruginosa* are often difficult to treat since it is resistant to a wide range of antibiotics due to multiple modes of resistance and its ability to form biofilms on medical devices (Lister et al. 2009; Langendonk et al. 2021). UTIs caused by *P. aeruginosa* are associated with high mortality in hospitalized patients (Lamas Ferreiro et al. 2017). *P. aeruginosa* biofilms are difficult to eradicate as bacteria embedded in the

matrix are protected from phagocytosis, are resistant to most drugs compared to their planktonic counterparts, and show long-term persistence (Thi et al. 2020). The biofilm-forming ability of *P. aeruginosa* is highly associated with its virulence and drug resistance.

The quantitative differences between biofilms formed by clinical isolates are categorized as strong, moderate, and weak biofilm producers (Stepanović et al. 2004). Owing to ease and relatively low cost, the crystal violet (CV) assay has been the most popular assay for the quantification of biofilms (O'Toole 2011; Thibeaux et al. 2020). A strong biofilm producer forms a thicker biofilm due to the presence of a high number of bacteria (either dead or alive or both) and the increased production of exopolymeric substances (Luther et al. 2018; Suriyanarayanan et al. 2018; Desai et al. 2019). Though several methods are available for biofilm quantification (Corte et al. 2019; Kragh et al. 2019), the CV assay is preferred, as it stains both live and dead cells, as well as the matrix and can be used as a primary indicator of biofilm-forming ability. The importance of distinguishing a strong biofilm producer from a weak biofilm producer can be linked to

CONTACT Devarshi Gajjar  devarshimistry@yahoo.com

 Supplemental data for this article is available online at <https://doi.org/10.1080/08927014.2022.2054703>.

This article has been republished with minor changes. These changes do not impact the academic content of the article.

© 2022 Informa UK Limited, trading as Taylor & Francis Group

their ability to survive in harsh conditions. For instance, increased amounts of matrix polymeric substances act as a shelter to protect the encased bacteria and dead cells in strong biofilms provide the necessary biomolecules for the remaining cells to survive (Webb et al. 2003; Ryder et al. 2007).

The composition of *P. aeruginosa* biofilms is well characterized in typed strains (PAO1 and PA14) and has been reviewed extensively (Mulcahy et al. 2014; Thi et al. 2020). The biofilm comprises an extracellular matrix having polysaccharides (alginate, pel, and psl), proteinaceous components, and extracellular DNA (eDNA). Studies on biofilm formation by *P. aeruginosa* in a CAUTI –murine model has shown biofilm formation can be mediated by eDNA even in the absence of exopolysaccharide (Cole et al. 2014). The biofilm matrix protein CdrA binds to pel and psl exopolysaccharides which increases the stability of biofilm (Reichhardt et al. 2018, 2020). The prevalence of *P. aeruginosa* in biofilms formed by bacteria on catheters has been documented (Xu et al. 2015; Tellis et al. 2017; Almalki and Varghese 2020) but a comparative analysis of the differences in the matrix components and biofilm-forming potential of these isolates are lacking.

The present study aimed to quantitate the differences in the biofilm-forming potential of *P. aeruginosa* isolates from UTIs. Further, biofilm formation on various catheters, adhesion, twitching motility, and arrangement of live-dead cells within the biofilm in strong and weak biofilm-producing isolates was also investigated.

Materials and methods

Bacterial cultures and growth conditions

All *P. aeruginosa* isolates were collected from the Sterling and Toprani pathology lab from Vadodara, Gujarat, India. *P. aeruginosa* isolates ($n=22$) were isolated from UTIs and maintained by subculturing on Pseudomonas Isolation Agar (PIA). Identification of isolates as *P. aeruginosa* was carried out using biochemical tests and 16S rRNA gene sequencing (data not shown)

Biofilm assay

Biofilm quantification of UTI-causing *P. aeruginosa* ($n=22$) and PAO1 was done using the crystal violet assay (Stepanović et al. 2004). Briefly, in a 96-well microtiter plate, 20 μ l of overnight grown culture (0.2 OD at 600 nm) and 230 μ l LB (Luria Broth) were

mixed and further incubated at 37°C for 24 h under static conditions. The next day, planktonic cells were removed and the biofilm was washed twice with normal saline, fixed with methanol for 15 min, and stained with 0.1% crystal violet (CV) for 15 min. The plates were air-dried for 15 min after being washed. The bound CV was dissolved in 33% glacial acetic acid and quantified spectrophotometrically at 570 nm. Based on cut-off O.D., isolates were classified as strong, moderate, and weak biofilm producers (Stepanović et al. 2004). The cut-off OD (OD_c) value was determined as three standard deviations above the mean OD of the negative control. Isolates were classified as no biofilm producer ($OD \leq OD_c$), weak biofilm producers ($OD_c < OD < 2 \times OD_c$), moderate biofilm producers ($2 \times OD_c < OD < 4 \times OD_c$), and strong biofilm producers ($4 \times OD_c < OD$). All the experiments were carried out in triplicate.

Growth curve

The growth curve was done for strong (ST-20, TP-25, TP-35, and TP-48) and weak (ST-22, TP-8, TP-10, and TP-11) biofilm producers using HT microtiter plate reader (Biotek Instruments, Winooski, VT, USA). 100 μ l of bacterial culture (OD at 600 nm \sim 0.05) was inoculated in a sterile 96-well flat-bottom microtiter plate and incubated at 37°C for 24 h. The optical density (OD) measurement was continuously measured at an interval of 15 min for 12 h until the culture reached to stationary phase. The growth curve was plotted and the growth rate was determined for each strain.

In vitro biofilm quantification on catheters

Experiments to examine biofilm quantification on catheters (silicone-coated latex and silicone catheters) were performed using four strong (ST-20, TP-25, TP-35, and TP-48) and weak (ST-22, TP-8, TP-10, and TP-11) biofilm producers. A 1 cm long piece of the catheter was cut vertically into 2 pieces, sterilized in methanol, and then air-dried. The catheter pieces were kept in a 24 well plate with 2 ml of 1:10 diluted (0.2 OD at 600 nm) culture and incubated at 37°C for 24 h. The amount of biofilm formed was quantified using a modified CV assay. The catheter was placed in a new plate, fixed with methanol for 15-min, stained with 0.1% CV; unbound CV was washed away twice with 0.85% NaCl, the plate was air-dried, bound CV was dissolved in 33% glacial acetic acid and CV was measured spectrophotometrically at

570 nm. Biofilm formed in the presence of Luria broth (LB), Natural Urine (NU) (obtained from a healthy volunteer, filter sterilized through a 0.2 μm filter, and stored at -20°C for further use) and Artificial urine (AU) (composition: 2.43% urea, 1% NaCl, 0.6% KCl, 0.64% Na_2HPO_4 , 0.05 mg mL^{-1} albumin, pH 7) were quantified using the same assay. For negative controls: LB, NU, and AU catheters without bacterial culture were used respectively. The experiment was performed in triplicate for each strain.

Light microscopy

The adhesion ability of the above-mentioned strong ($n=4$) and weak ($n=4$) biofilm producers was examined. Briefly, 5 ml of 1:10 diluted bacterial culture (0.2 OD at 600 nm) in LB medium was inoculated in 6 well plates with coverslips and incubated at 37°C for 4 h under static conditions. After incubation, the unbound cells were washed off with 0.85% NaCl, Gram-stained, and observed under a microscope (BX 51 Olympus microscope, Japan) at 100X magnification. The number of cells adhered to the coverslip was counted using Fiji software.

Twitching motility

Twitching motility for previously mentioned strong ($n=4$) and weak ($n=4$) biofilm-producers was determined on 1% Luria agar (LA) plates by inoculating and incubating them at 37°C for 24 h followed by measuring the twitching zone (Darzins 1993). Further confirmation of twitching motility was done by phase-contrast time-lapse microscopy. Briefly, twitching motility was observed by spotting 1 μl (0.2 OD at 600 nm) of bacterial culture on a 1% LA pad (we ensured that the LA pad was air-dried). The twitching motility was observed for 4 h and 24 h. The experiment was done in biological triplicates.

Gene expression quantification of type 4 pili and *cdr A* gene

The levels of expression of type 4 pili and biofilm matrix protein Cdr A genes listed in the supplementary data (Table S1) were analyzed from 4 h to 24 h old biofilms. RNA extraction was carried out using a Nucleospin RNA kit (Macherey Nagel, Hoerdt, France). RNA integrity was checked on 2% gel and quantification was done using a Nanodrop (Thermo Fisher Scientific, Waltham, MA, USA). First-strand

cDNA synthesis was performed using a prime 1st Strand cDNA synthesis kit (Takara, Bio Inc, Japan). The qPCR cycling conditions were as follows 95°C for 5 min and 40 cycles of 30 s at 95°C , 30 s at 57°C . Relative quantification was carried out from three independent biological replicates. Data were normalized to *rpo D* gene expression and fold changes were calculated according to the $2^{-\Delta\Delta\text{Ct}}$ method. The fold change of strong biofilm producers was normalized to weak biofilm producers.

Confocal laser scanning microscopy (CLSM)

Using a Carl Zeiss CLSM 780 and 710 microscope, 24 h old biofilm formed on coverslips in LB medium in 6 well culture plates was examined. Before staining, biofilm was rinsed with 1 ml of 0.85% NaCl to remove planktonic cells. The remaining biofilm attached to the coverslip was stained with Syto 9 and PI dye from LIVE/DEAD[®] BacLight[™] Bacterial Viability Kit for 10 min. The excess stain was gently washed away with 0.85% NaCl. 3D structure of biofilm was captured by CLSM using Z stack. Fiji software was used to measure the live and dead cells in images.

Field emission gun scanning electron microscopy (FEG-SEM)

Strong (TP-25) and weak (TP-8) biofilm producers were cultured in LB for 24 h at 37°C on a silicone-coated latex catheter, as stated above. After incubation, the biofilm was rinsed with sterile PBS (Phosphate Buffer Saline), fixed with 2% glutaraldehyde in PBS at 4°C overnight, then sequentially dehydrated with 30, 50, 70, 90, and 100% ethanol in order. FEG-SEM (Nova Nano SEM 450, FEI Ltd., Hillsboro, OR, USA) was performed in environmental mode.

Quantification of biofilm matrix components

With few modifications, eDNA and extracellular protein quantification were done as described by (Wu and Xi 2009) and normalized with OD 600 nm. In 24 well plates, 2 ml of 1:10 diluted (0.2 at OD 600 nm) culture in LB medium was incubated at 37°C for 24 h. The next day, biofilm was gently rinsed with 0.85% NaCl to remove planktonic cells before being resuspended in 1 ml of 0.85% NaCl. Biofilm was homogenized by vortexing for 30 s and cells were removed by passing it through a 0.22 μm filter. 500 μl of filtered suspension was used for eDNA

quantification and the remaining was used for protein quantification.

eDNA quantification

The eDNA was extracted from 500 μl of filtered solution (above) using the phenol-chloroform method as previously described (Wu and Xi 2009) and quantified by measuring absorbance at 260 nm using nanodrop (Thermo Fisher Scientific, Waltham, MA, USA). The OD at 600 nm was used to normalize the eDNA quantification.

Extracellular protein quantification

Extracellular protein was quantified using a Bradford assay by measuring absorbance at 595 nm in a microtiter plate reader (Multiskan Go, Thermo Fisher Scientific, Waltham, MA, USA). Briefly, 100 μl of filtered solution was added to 1000 μl of Bradford reagent and incubated at room temperature for 10 min. Absorbance was measured at 595 nm.

Pel polysaccharide quantification

The amount of Congo red that binds to Pel-dependent EPS was assayed as described by Madsen et al. 2015 (Madsen et al. 2015). Briefly, 1:10 diluted (0.2 OD at 600 nm) overnight grown culture was inoculated in 2 mL LB and incubated at 37 °C for 24 h. Bacterial content along with EPS was pelleted by centrifugation, resuspended in 40 mg mL⁻¹ Congo red in 1% LB and incubated for 2 h at 37 °C at 250 rpm. After 2 h, EPS was pelleted *via* centrifugation and the absorbance of the supernatants of each suspension was measured at 490 nm. 1% LB with 40 mg mL⁻¹ Congo red was used as a blank.

Alginate quantification

Alginate extraction was carried out following the protocol by Jones et al., 2013 (Jones et al. 2013). Briefly, a 24 h bacterial colony was scraped off the plate, resuspended in 0.85% NaCl, and collected by centrifugation (12,000 $\times g$ for 30 min). The supernatant was treated with 2% Cetyl Pyridium chloride and alginate was collected by centrifugation. The pellet was resuspended in 1 ml of 1 M NaCl, precipitated with cold isopropanol, and resuspended in normal saline. Alginate quantification was determined by carbazole assay (Cesaretti et al. 2003) with 96 well format modifications (Knutson and Jeanes 1968). 50 μl

of resuspended alginate was treated with a 200 μl borate-sulfuric acid reagent (10 mM H₃BO₃ in concentrated H₂SO₄) at 100 °C for 15 min. Further, 50 μl of carbazole reagent (0.1%) was added and heated to 100 °C for 10 min. Absorbance was measured at 550 nm (Multiskan Go, Thermo Fisher Scientific, Waltham, MA, USA). Seaweed alginate was used as a standard to determine the concentration of alginate.

Pyocyanin quantification

Pyocyanin production by strong ($n=4$) and weak ($n=4$) biofilm producers were determined as described by (Essar et al. 1990). Briefly, overnight grown culture was 1:10 diluted (0.2 OD at 600 nm) and inoculated in 2 ml LB medium and kept shaking at 37 °C for 24 h. The next day, the culture was centrifuged, pyocyanin was extracted from the supernatant with 3 ml chloroform and then re-extracted with 0.2 N HCl. By measuring absorbance at 520 nm and multiplying it by 17.072, the concentration can be expressed as a microgram of pyocyanin produced per ml of supernatant. The OD at 600 nm was used to normalize the concentration. The experiment was performed in triplicate using a blank of 0.2 N HCl.

Rhamnolipid quantification

In LB, 1:10 diluted (0.2 OD culture at 600 nm) overnight grown culture was inoculated and kept at 37 °C for 24 h. Four ml of the supernatant pH was adjusted to 2.3 \pm 0.2 using 1 N HCl and extracted with 5 volumes of chloroform. To 4 ml of chloroform extract, 200 μl of 1 g L⁻¹ methylene blue solution (pH of methylene blue was adjusted to 8.6 \pm 0.2 by adding 50 mM Borax buffer) and 4.9 ml distilled water was added. The sample was vigorously mixed and kept at room temperature for 15 min. The OD of the chloroform phase was measured at 638 nm and normalized with the A_{600nm} (Pinzon and Ju 2009). Chloroform was used as blank.

Effect of exogenous treatments (enzymes, eDNA, proteins) on biofilm formation

Enzymatic digestion of biofilm

Biofilm was grown in a 96 well microtiter plate for 24 h at 37 °C as described for the biofilm assay. The next day, planktonic cells were washed off with 0.85% NaCl and the biofilm was treated with 100 $\mu\text{g ml}^{-1}$ of DNase, RNase, and proteinase K each in separate wells and further incubated at 37 °C for 24 h (Tetz

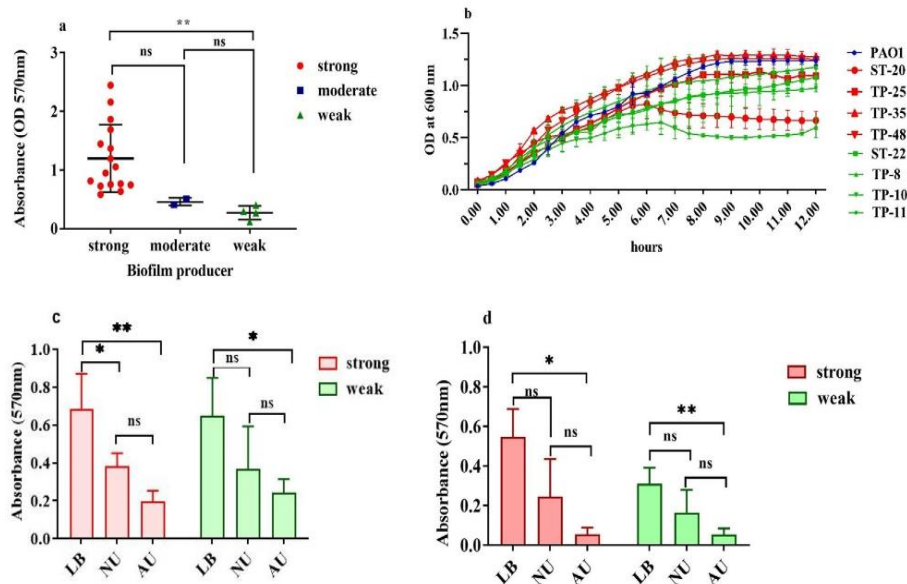


Figure 1. Biofilm Quantification: Biofilm quantification and categorization of UTI isolates of *P. aeruginosa* ($n=22$) into strong, moderate and weak (a). Growth curve of strong (ST-20, TP-25, TP-35, TP-48) and weak biofilm producers (ST-22, TP-8, TP-10, TP-11) (b). Biofilm quantification on silicone-coated latex catheter in presence of LB, NU, AU (c) and silicone catheter in presence of LB, NU, AU (d). The experiment was conducted in three biological replicates for each strain. Error bars indicate standard deviation. Two-way ANOVA was performed for statistical significance were ns $p > 0.05$, * $p < 0.05$, ** $p < 0.005$, *** $p < 0.0005$.

et al. 2009). Following 24h, the biofilm was rinsed with 0.85% NaCl and quantified using the crystal violet assay. LB medium with culture was used as control and sterile LB medium was used as the blank. The experiment was performed in triplicate.

Addition of eDNA and extracellular protein in biofilm

To substantiate the role of eDNA and extracellular protein in biofilm, an addition assay was performed (Harmsen et al. 2010). Biofilm was formed using the above mention protocol with the addition of *P. aeruginosa* extracted eDNA, genomic DNA, and extracellular protein (concentration 100 ng mL^{-1} for DNA and $3 \mu\text{g mL}^{-1}$ for protein) and incubated at 37°C for 24 h (Harmsen et al. 2010). The next day, unbound cells were washed off and a CV assay was performed as stated previously. Bacterial culture with LB was used as control and only LB as blank. The experiment was performed in triplicate.

Statistical analysis

Statistical analysis for biofilm formation on catheters was done using the GraphPad Prism 9.0 software with two-way ANOVA. For other experiments

represented by bar graphs and line graphs, student's *t*-test and one-way ANOVA or 2-way ANOVA was applied. Non-parametric data represent the mean \pm standard deviation.

Results

Biofilm categorization of UTI isolates of *P. aeruginosa*

The crystal violet (CV) assay was used to categorize UTI-causing *P. aeruginosa* ($n=22$) isolates into strong, moderate, and weak biofilm producers based on cut-off OD value. The majority of the isolates were found to be strong ($n=16$), while few were moderate ($n=2$) or weak ($n=4$) biofilm producers (Figure 1a). Strong (ST-20, TP-25, TP-35 and TP-48) and weak (ST-22, TP-8, TP-10, TP-11) biofilm producers were randomly selected for all further experiments. The mean growth rate of strong ($n=4$) and weak ($n=4$) biofilm producers was 0.24 ± 0.02 per hour (Figure 1b). One isolate of each strong (ST-20) and weak (TP-11) biofilm producer appeared as slow growers and showed a lower plateau but did not attain statistical significance (Figure 1b).

Biofilm quantification on catheters

In vitro biofilm quantification was studied on silicone-coated latex and silicone catheters in presence of LB, NA, and AU of strong (ST-20, TP-25, TP-35 and TP-48) and weak (ST-22, TP-8, TP-10, TP-11) biofilm producers. On both catheters, the maximum amount of biofilm formation was observed on LB followed by NU and AU by strong and weak biofilm producers (Figure 1c-d). There was no difference in biofilm formation by strong biofilm producers on silicone-coated latex compared to silicone catheters irrespective of the medium used (Figure S1a). Within weak biofilm producers, the highest biofilm formation was observed on silicone-coated latex catheters compared to silicone in the presence of LB (Figure S1a). Negligible differences were observed in NU and AU (Figure S1a). Further, the maximum amount of biofilm formation was observed by strong biofilm producers compared to weak biofilm producers on silicone catheters in LB (Figure S1b). Whereas no difference was observed in biofilm formation by strong and weak biofilm producers on both catheters irrespective of the medium used (Figure S1b).

Adhesion assay and twitching motility

The cell adhesion ability of strong and weak biofilm producers was examined on coverslips after 4 h of incubation. Adhesion by strong biofilm producers showed a greater number of cells adhered to the coverslip compared to weak biofilm producers in light microscopy images (Figure 2a). The number of cells adhered to the coverslip was significantly high in strong ($n = 727 \pm 100$) biofilm producers when compared with weak ($n = 127 \pm 29$) biofilm producers (Figure 2b). Type 4 pili (T4P) mediated twitching motility is essential for surface attachment and the initial stage of microcolony formation.

The twitching motility of PAO1 and strong and weak biofilm producers on 1% LA plates was examined (Figure 2c). A significant difference was observed between the twitching zone of strong (1.1 ± 0.40 mm) and weak (0.6 ± 0.21 mm) biofilm producers (Figure 2d). Further, in phase-contrast time-lapse microscopy, a greater number of twitching cells were observed at 4 h in strong biofilm producers (Video S1—upper panel). In contrast, the twitching of cells was less in weak biofilm producers (Video S1—lower panel). One isolate namely TP10 (weak biofilm producer) completely lacked twitching motility (Video S1—lower panel TP10). As a consequence of greater twitching in strong biofilm producers, the wrinkly edge formation

was observed at 24 h (Figure 2e, upper panel). The fully wrinkly colony edge formation was absent in weak biofilm producers (Figure 2e, lower panel). The quantification of gene expression for the T4P gene was done at 4 h and 24 h biofilms. The type 4 pili expression was 5-fold more compared to weak biofilm producers at 4 h (Figure 2f), and 3-fold high at 24 h (Figure 2f).

Microscopy of biofilm

The biofilm formed on the coverslips by strong and weak biofilm producers was visualized by CLSM using Syto and PI dyes. The arrangements of live and dead cells within the biofilms formed by strong and weak biofilm producers can be viewed in the orthogonal plane (Figure 3 a and c). The biofilm formed by strong biofilm producers had less live cells and a greater number of dead cells as observed in the orthogonal plane (Figure 3a). While biofilm formed by weak biofilm producers had more live cells except for one isolate (TP-11) (Figure 3c) in which excess cell death was observed. This could be because of more pyocyanin production (in TP11), as pyocyanin-mediated cell death is reported in *P. aeruginosa* (Das and Manefield 2012). Further, the YZ and XZ planes of Figure 3a and c showed the variation across the thickness in biofilms formed by strong ($31.25 \mu\text{m} \pm 14.3$) and weak ($19.05 \mu\text{m} \pm 9$) biofilm producers (Figure 3 a and c). The tiled images of strong biofilm producers show tightly packed cells (Figure 3 b) whereas in weak biofilm producers, cells are loosely distributed across the substratum (Figure 3 d). Representative supplementary video S2 shows a clear arrangement of live and dead cells within the biofilm. Biofilms formed by strong biofilm producers are densely packed with dead bacteria confined near the substratum, whereas live cells are scarce and positioned above dead cells (Supplementary Video S2—upper panel). However, the biofilm formed by weak biofilm producers differs in arrangements of live and dead cells. The biofilm formed by weak biofilm producers (ST-22 and TP-10) had more live cells near the substratum than dead cells (Supplementary Video S2—lower panel). Additionally, the number of dead and live cells in each slice of Z stack from strong ($n = 4$) and weak ($n = 4$) biofilm producers were determined. Cell counts (total and dead) show significant differences between strong ($n = 4$) and weak ($n = 4$) biofilm producers (Figure 3e).

FEG-SEM at 3000X resolution of biofilm formed on silicone-coated latex catheter in the presence of LB

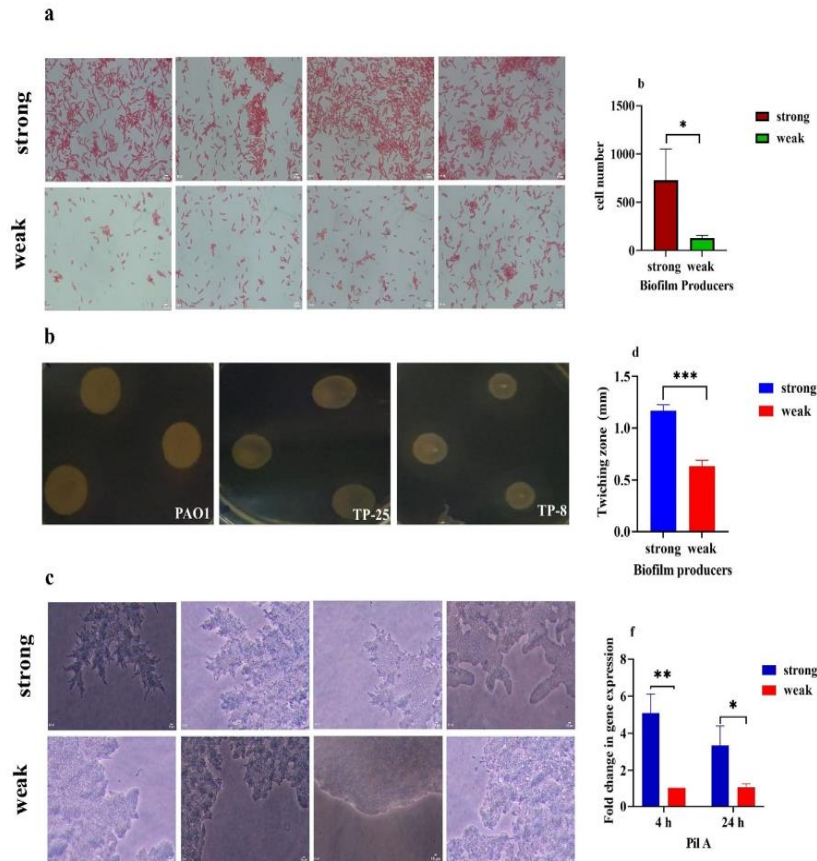


Figure 2. Cell adhesion and twitching motility: Representative images of light microscopy of strong (ST-20, TP-25, TP-35, TP-48) and weak (ST-22, TP-8, TP-10, TP-11) biofilm producers adhered to coverslip at 4 h incubation (a). Cell count of adhesion assay (b). Twitching motility zone of PAO1, strong (TP-25) and weak (TP-8) biofilm producers on 1% LA pad (c). Twitching zone diameter of strong and weak biofilm producers (d). Phase-contrast microscopy of colony edge formation at 24 h of strong ($n=4$) and weak ($n=4$) biofilm producers (e). Pil A gene expression of strong and weak biofilm producers at 4 h and 24 h. All experiments were performed in triplicate for each isolate (f). Statistical significance from student *t*-test were * $p < 0.5$, ** $p < 0.05$, *** $p < 0.005$. Scale bar indicates 10 μm .

medium shows that strong (TP-25) produced thick biofilm (Figure 4a upper left panel). Due to the EPS, bacteria were not visible at 3000X in the biofilm formed by a strong biofilm producer. On the other hand, biofilm formed by weak biofilm producers had a thin layer of bacteria adhered to the catheter and less EPS (Figure 4b upper right panel). Increased magnification to 6000X showed rod-shaped cells encased within the EPS matrix of biofilm formed by strong biofilm producer (Figure 4a; middle left panel); whereas in biofilm formed by weak biofilm producers, cells are adhered to the catheter as well as to each other and EPS production is hardly observed (Figure 4b; middle right panel). Further magnification to 12000 X, also confirmed that cells are encased in EPS

of strong biofilm producer (Figure 4a lower left panel) and the EPS looked like a dense mass with an irregular surface. While in weak biofilm producers, cells aggregated and microcolony formation was barely observed (Figure 4b; lower right panel).

Components of biofilm

The difference in biofilm components: eDNA, an extracellular protein, pyocyanin, rhamnolipid, pel, and alginate exopolysaccharide was measured for biofilms formed by strong ($n=4$) and weak biofilm producers ($n=4$). The amount of eDNA was $265 \pm 130 \mu\text{g}$ at OD600 in strong biofilm producers and it was $44.96 \pm 11.45 \mu\text{g}$ at OD600 weak biofilm producers

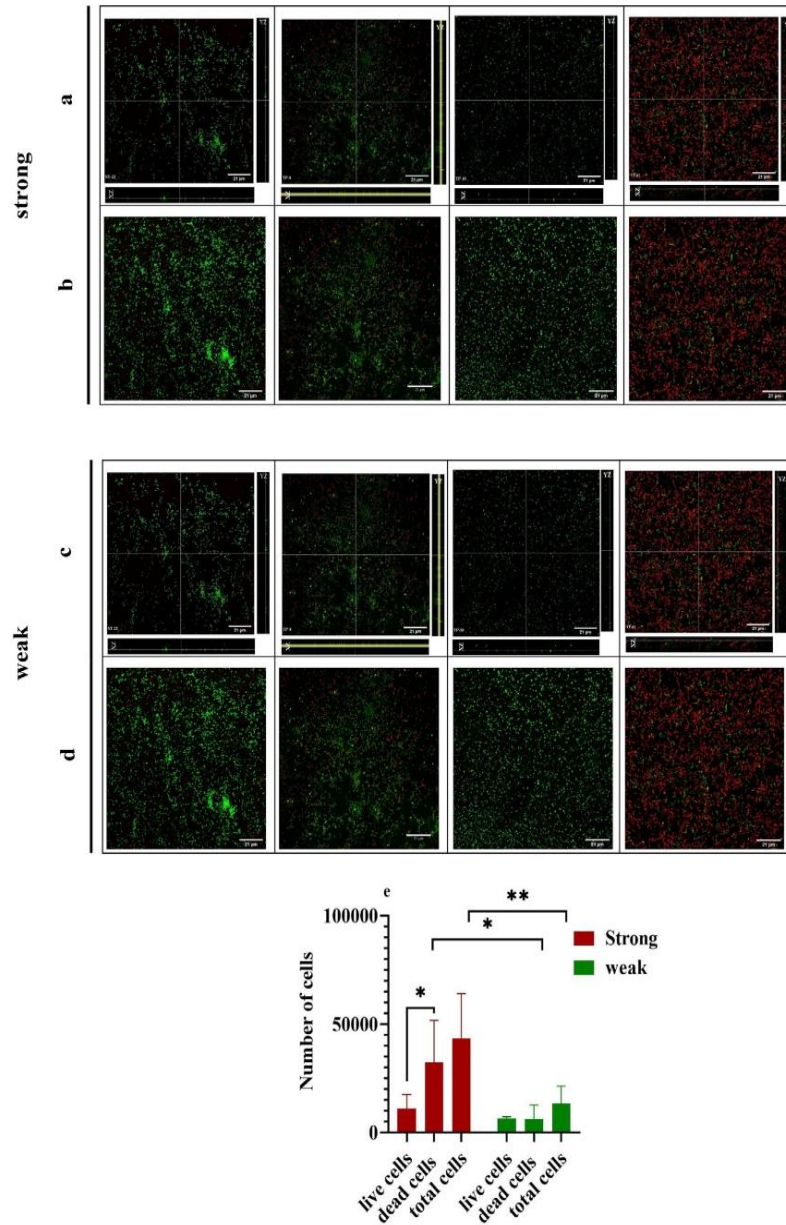


Figure 3. Confocal laser scanning microscopy (CLSM) of biofilms formed by strong and weak biofilm producers: Biofilm formed by strong (ST-20, TP-25, TP- 35, TP-48) and weak (ST-22, TP-8, TP- 10, TP-11) biofilm producers on coverslip after 24 h were subjected to CLSM after staining with Syto9 (green – live cells) and PI (red – dead cells) (a, b, c, and d). Representative images of orthogonal view of Z-stack strong (a-) and weak (c-) biofilm producers, tiled images of strong (b) and weak (d) biofilm producers. Cell counts of living, dead, and total cells (dead and live) within the Z-stack of strong and weak biofilm producers (e). One-way ANOVA was carried out for statistical significance were ns $p > 0.05$, * $p < 0.05$, ** $p < 0.005$. Scale bar indicates 21 μm .

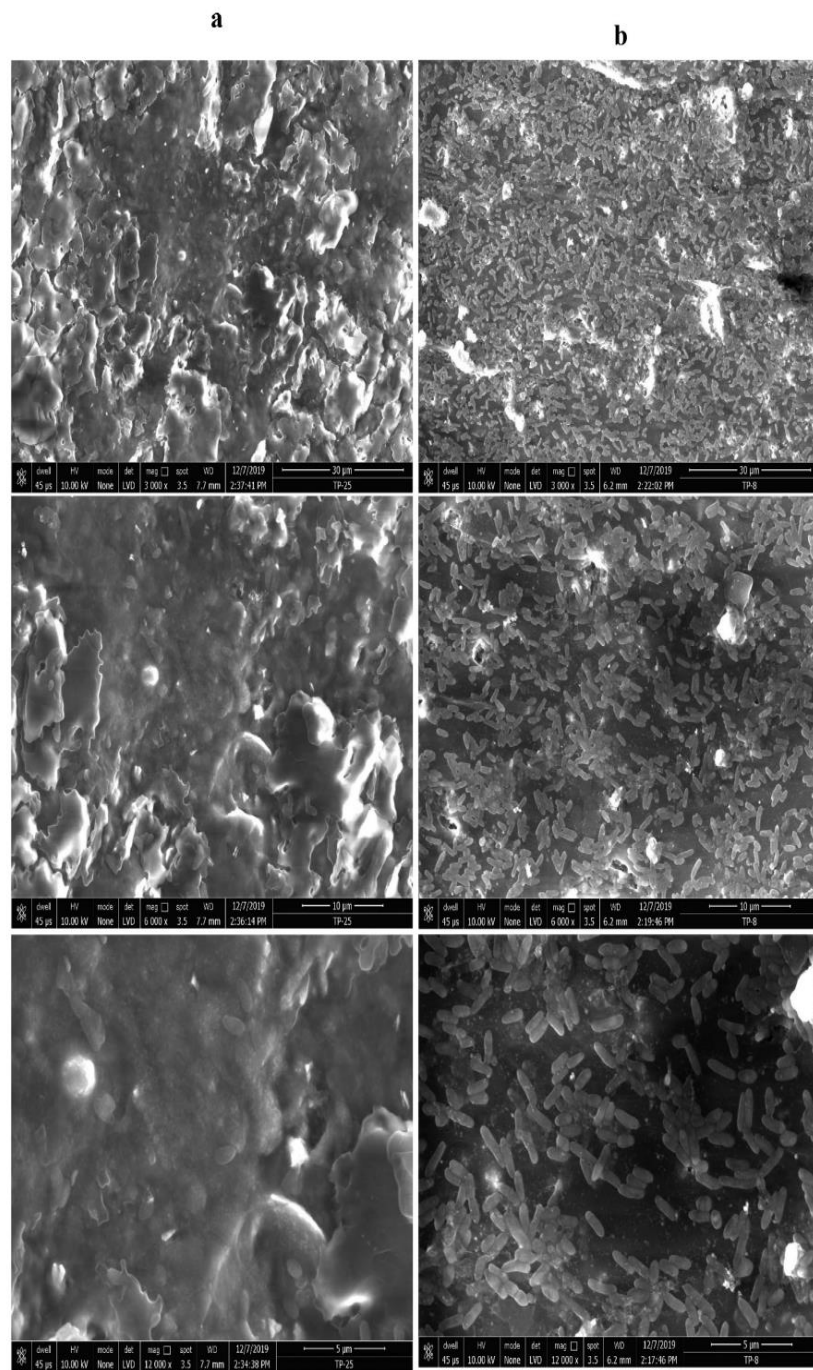


Figure 4. FEG-SEM of biofilm: Representative images of biofilm formed by strong (TP-25) (a) and weak (TP-8) (b) biofilm producers on silicone-coated latex catheter at 3000X (upper panel), 6000X (middle panel), and 12000X (lower panel) magnifications. Scale bar indicates 30 μm, 10 μm, 5 μm.

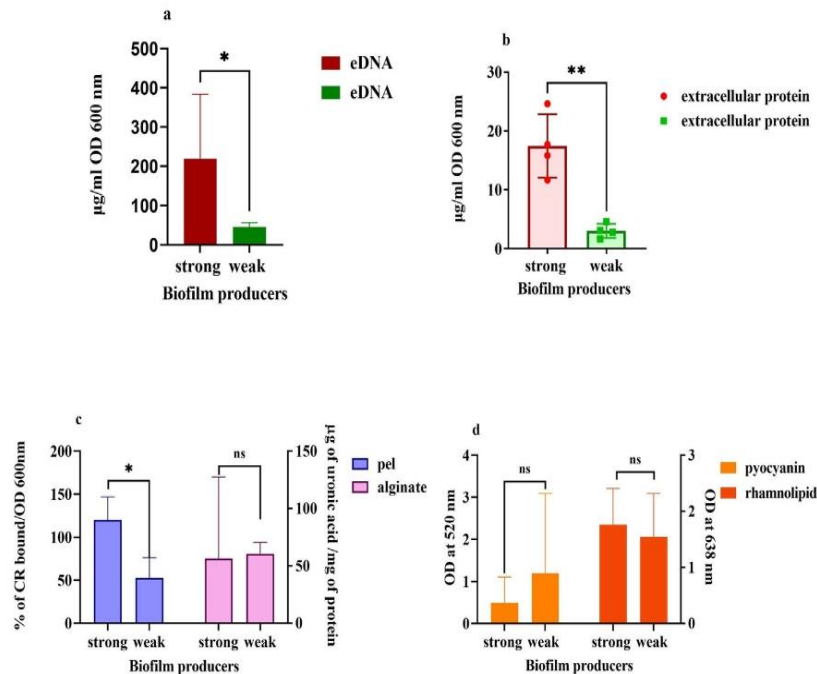


Figure 5. Quantification of biofilm matrix components: eDNA (a), extracellular protein (b) pel and alginate exopolysaccharide (c), rhamnolipid and pyocyanin (d). Error bar indicates standard deviation. Student *t*-test carried out for statistical significance were ns $p > 0.05$, * $p < 0.05$, ** $p < 0.005$.

(Figure 5a). The extracellular protein quantified in biofilm formed by strong biofilm producers ($17.45 \pm 5.30 \mu\text{g}$ at OD600) was also significantly higher than weak biofilm producers ($3.04 \pm 1.20 \mu\text{g}$ at OD600) (Figure 5b). The concentration of pel exopolysaccharides was significantly higher in strong biofilm producers ($120.10 \pm 26.79 \mu\text{g}$ at OD600) than weak biofilm producers ($52.83 \pm 23.38 \mu\text{g}$ at OD600) (Figure 5c). There was no significant difference between strong and weak biofilm producers in the case of alginate exopolysaccharide, pyocyanin, and rhamnolipid (Figure 5c-d).

Effect of exogenous treatments (enzymes, eDNA, proteins) on biofilm formation

The effect of enzymatic treatments (DNase I, proteinase K, and RNase) on biofilm formation by strong biofilm producers showed the greatest inhibition by proteinase K treatment, followed by RNase and DNase treatment that reduced biofilm by 76.35%, 63.43%, and 43.35%, respectively (Figure 6a). Out of the three treatments, only the DNase treatment resulted in a significant reduction of biofilm (58.27%) in weak biofilm producers (Figure 6a). Further, the

addition of exogenous DNA and extracellular protein may increase the amount of biofilm. A decrease in biofilm was observed in both strong and weak biofilm producers upon the addition of eDNA when compared to control (no eDNA is added) (Figure 6b). No significant difference was observed with the addition of extracellular protein in comparison to the control (no extracellular protein added) (Figure 6c)

Discussion

The first objective in the present study was to determine whether the UTI isolates of *P. aeruginosa* had any differences in their biofilm-forming abilities. The majority of isolates were strong biofilm producers with negligible differences in biofilm formation between silicone and silicone coated catheters; all isolates showed levels of biofilm production on catheters in order of LB > NU > AU medium. Similar results were observed by Vipin et al., 2019 who showed that weak biofilm producers form strong biofilms on silicone-coated latex catheters in tryptone soya broth (Vipin et al. 2019). The porous surface of silicone-coated latex catheters was shown to enhance biofilm formation due to the high adhesion of bacteria (Lee

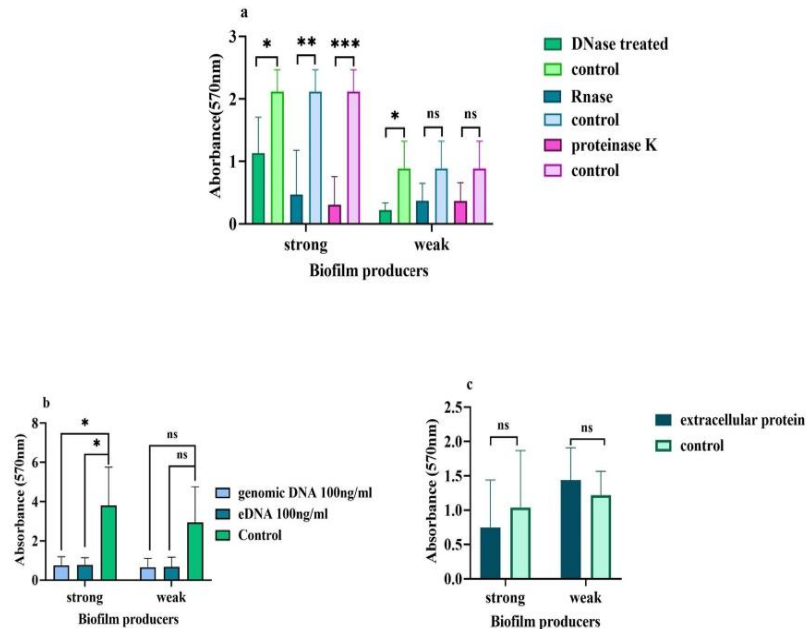


Figure 6. Effect of exogenous treatments (enzymes, eDNA, proteins) on biofilm formation: Effect of DNase I, RNase and proteinase K (a); Addition of eDNA and genomic DNA (b); addition of extracellular protein (c). Statistical significance carried out using student t-test were ns $p > 0.05$, * $p < 0.05$, ** $p < 0.005$, *** $p < 0.0005$.

et al. 2017), while silicone catheters have a smooth surface and are known to reduce cell adhesion (Feneley et al. 2015). In a recent study, *P. aeruginosa* exhibited significantly high biofilm when cultured on a 96-well polystyrene plate (hydrophobic surface) and glass surface in the presence of LB medium (Asghari et al. 2021). A limitation of the study is that the entire study is based on the initial categorization of biofilm formation into strong and weak biofilm producers using the CV assay in 96 well polystyrene plates. CV staining probes all components of the biofilm (i.e. live-dead cells, proteins, RNA, eDNA, polysaccharides, etc.) and so it was used as a preliminary indicator. Later, microscopy (light, CLSM, and SEM) and biochemical assays were done to find the differences between biofilms formed by strong and weak biofilm producers. Hence, glass coverslips were used for adhesion assays and CLSM imaging, while silicone-coated latex catheters were used for SEM. Many variables like surface properties, cell surface hydrophobicity, medium, cell appendages (flagella and T4P) (Zheng et al. 2021) could contribute to the diverse behaviour of clinical isolates. Diverse behaviour is also reported for isolates causing cystic fibrosis (Deligianni et al. 2010). Only 54% of keratitis causing *P. aeruginosa*

isolates showed biofilm formation (Heidari et al. 2018). Most studies on *P. aeruginosa* from UTI have focused on antibiotic resistance (Saxena et al. 2014; Kamali et al. 2020; Mirzahosseini et al. 2020) and reports on the quantification of biofilm formation by clinical isolates of *P. aeruginosa* causing UTIs are scanty.

The differences in biofilms formed by clinical isolates could be due to their differences in twitching motility, adhesion and/or components of the biofilm matrix. Cell adhesion, twitching motility, and expression of *pilA* gene were higher in strong biofilm producers. The importance of type 4 pili (T4P) mediated twitching motility as a means of initiating contact on abiotic surfaces and biofilm formation is well documented (O'Toole and Kolter 1998; Pratt and Kolter 1998; Mattick 2002). In a study on clinical and environmental isolates, it was found that when the motility phenotype was present, there was a notable increase in biofilm (Head and Yu 2004; Inclan et al. 2011). Differences in biofilm formation and variations in biofilm morphology amongst clinical isolates ($n=5$) from cystic fibrosis patients were correlated with motility and it was concluded that though motility is not an absolute requirement for biofilm formation it

does contribute to the formation of thick biofilms (Deligianni et al. 2010). In a recent study of 190 clinical isolates of *P. aeruginosa*, twitching motility was strongly associated with high biofilm formation while isolates with high swimming and swarming motility failed to produce a strong biofilm (Horna et al. 2019). The biogenesis, functioning, and regulation of T4P mediated twitching motility is well characterized and several complex systems control the T4P responses. Hence, prediction of T4P behavior in response to diverse cues is difficult. The two major determinants of the motility–sessility switch in *P. aeruginosa* are the cellular levels of c-di-GMP or cAMP, and levels of both have shown to increase during growth on solid media (Hengge 2009; Römling et al. 2013; Valentini and Filloux 2016). Levels of c-di-GMP and cAMP are adjusted in response to extracellular signals received by several sensing systems (WspA, WspR, Gac-Rsm, RocS1) and chemotactic cluster (PilGHJK-ChpABC) respectively (Chang 2017). In a recent study, T4P mediated motility was shown to cause biofilm expansion in response to host-derived signals, serum albumin (known to be present in urine) and mucin (elevated in lungs of cystic fibrosis patients). BSA, mucin, and tryptone were shown to elevate levels of T4P and cAMP *via* ChpC (Nolan et al. 2020). The same study also showed that secreted protease activity may be required for liberating components from mucin, BSA, and tryptone that stimulate twitching motility and that a small quantity of this component is present in tryptone that does not require protease activity to get liberated. High biofilm formation in LB was observed (tryptone: 10 g L⁻¹); hence it is hypothesized that the presence of tryptone could increase the amount of cAMP thereby causing strong biofilm formation. On the other hand, the presence of urea in natural and artificial urine may inhibit quorum sensing due to which biofilm formation was less in presence of urine (Cole et al. 2018). Overall, a vast range of environmental and host signals have been shown to stimulate twitching and these signals along with the genomic diversity of clinical isolates lead to differences in biofilm formation among clinical isolates of *P. aeruginosa*.

Increased cell death, eDNA, an extracellular protein, and pel polysaccharide in biofilms formed by strong biofilm producers was observed. Association of cell death with eDNA in *P. aeruginosa* biofilms is very well established and cell death in *P. aeruginosa* biofilms is considered analogous to programmed cell death in eukaryotes. The considerable amount of DNA in the biofilm matrix is mediated due to cell

autolysis in microcolonies (Webb et al. 2003). Pel is a cationic exopolysaccharide produced by *P. aeruginosa*, and it has been shown to cross-link extracellular DNA in the biofilm matrix to provide stability and structural integrity to the biofilm (Jennings et al. 2015). Mechanisms of cell death and eDNA release have been reviewed recently (Sarkar 2020). These include; membrane damage (caused due to quorum sensing molecules and pyocyanin production), lambda prophage induction and reinfection, ROS production and PQS mediated Phz A-G expression. One of many of the above mechanisms could contribute to cell death and eDNA in biofilms. Hence, further studies to clarify the possible involvement of the above pathways for cell death are warranted using the clinical isolates. Increased production of pyocyanin in TP-11 (weak biofilm producer) may be responsible for increased cell death. It appears that cell death alone may not contribute to strong biofilm formation. One limitation of this study is that exopolysaccharide Psl was not measured. The exopolysaccharide Psl is cell-surface associated and functions as an adhesin in the initial phase of biofilm formation, but relocates as a peripheral exopolysaccharide at later stages of biofilm formation (Ma et al. 2009). *P. aeruginosa* isolates with the pel and psl genes had more robust biofilms than strains deficient in these genes; in a murine model, cell lysis is mediated by urea, and biofilm formation is independent of exopolysaccharides (Cole et al. 2014).

The cdr A is the only well-characterized extracellular protein (Reichhardt et al. 2020) and in the present study, no difference was found in the expression of cdr A when compared between strong and weak biofilm producers (data not shown). It is possible that the protein content in the matrix is highly dynamic and consists of many proteins. A study using iTRAQ-based quantitative proteomics to evaluate matrix-associated proteins isolated from different phases of *P. aeruginosa* ATCC27853 biofilms showed that 54 different proteins varied from time to time during biofilm formation (Zhang et al. 2015). This warrants further studies on extracellular proteins in biofilms caused by *P. aeruginosa* in CAUTIs.

Based on these results, high adhesion ability and twitching motility contribute to strong biofilm formation. Weak biofilm-producing isolates showed good diversity. Since biofilms are difficult to eliminate, twitching motility and high adhesion ability found in the early stages of biofilm formation can be exploited as therapeutic targets for biofilm formation.

Acknowledgments

We would like to acknowledge “Confocal Laser Scanning Microscopy (Carl Zeiss LSM 780) Central Facility of IRCC” housed in the BSBE Department of IIT-Bombay. We also acknowledge “Confocal Laser Scanning Microscopy (Carl Zeiss LSM 710) housed in Central Facility at VSI-CMB Department of MSU Baroda”. We thank the Sophisticated Instrumentation Centre for Applied Research and Testing-SICART, Vallabh Vidyanagar for their Scanning Electron Microscope (SEM) facility.

Disclosure statement

The authors declare no conflict-of-interest disclosure.

Supplementary material

Table S1: Primers used in the study for Pili A and Cdr A gene expression in strong and weak biofilm forming isolate.

Supplementary Figure S1: Statistical comparison of biofilm formation by strong and weak biofilm producers (a and b). The Experiment was conducted in three biological experiments for each strain. Error bar indicates standard deviation. Two-way ANOVA was performed for statistical significance were ns $p > 0.05$, * $p < 0.05$, ** $p < 0.005$, *** $p < 0.0005$.

Supplementary video S1: Twitching motility of strong and weak biofilm producers at 4 h on 1% LA pad.

Supplementary video S2: CLSM image of biofilm formed by strong and weak biofilm producers.

Funding

This work was supported by a research grant from Maharaja Sayajirao University of Baroda (RCC/Dir/2017/335/10). Hiral Patel thanks for CSIR-UGC fellowship-University Grants Commission (UGC). We are also grateful for the infrastructure support to this department under the DST-FIST program of the Government of India and Biotechnology- Teaching Programme.

ORCID

Devarshi Gajjar  <http://orcid.org/0000-0002-1330-3823>

References

- Almalki MA, Varghese R. 2020. Prevalence of catheter associated biofilm producing bacteria and their antibiotic sensitivity pattern. *J King Saud Univ Sci.* 32:1427–1433. doi:10.1016/j.jksus.2019.11.037
- Asghari E, Kiel A, Kaltschmidt BP, Wortmann M, Schmidt N, Hüsgen B, Hütten A, Knabbe C, Kaltschmidt C, Kaltschmidt B. 2021. Identification of microorganisms from several surfaces by maldi-tof ms: *P. aeruginosa* is leading in biofilm formation. *Microorganisms.* 9: 918–992. doi:10.3390/microorganisms9050992
- Cesaretti M, Luppi E, Maccari F, Volpi N. 2003. A 96-well assay for uronic acid carbazole reaction. *Carbohydr Polym.* 54:59–61. doi:10.1016/S0144-8617(03)00144-9
- Chang C. 2017. Surface sensing for biofilm formation in *Pseudomonas aeruginosa*. *Front Microbiol.* 8:2671. doi: 10.3389/fmicb.2017.02671
- Cole SJ, Hall CL, Schniederberend M, Farrow JM, Goodson JR, Pesci EC, Kazmierczak BI, Lee VT. 2018. Host suppression of quorum sensing during catheter-associated urinary tract infections. *Nat Commun.* 9:1–8. doi:10.1038/s41467-018-06882-y
- Cole SJ, Records AR, Orr MW, Linden SB, Lee VT. 2014. Catheter-associated urinary tract infection by *Pseudomonas aeruginosa* is mediated by exopolysaccharide-independent biofilms. *Infect Immun.* 82:2048–2058. doi:10.1128/IAI.01652-14
- Corte L, Pierantoni DC, Tascini C, Roscini L, Cardinali G. 2019. Biofilm specific activity: a measure to quantify microbial biofilm. *Microorganisms.* 7:73. doi:10.3390/microorganisms70300
- Darzens A. 1993. The pilG gene product, required for *Pseudomonas aeruginosa* pilus production and twitching motility, is homologous to the enteric, single-domain response regulator CheY. *J Bacteriol.* 175:5934–5944. doi: 10.1128/jb.175.18.5934-5944.1993
- Das T, Manefield M. 2012. Pyocyanin promotes extracellular DNA release in *Pseudomonas aeruginosa*. *PLoS One.* 7:e46718. doi:10.1371/journal.pone.0046718
- Deligianni E, Pattison S, Berrar D, Ternan N, Haylock R, Moore J, Elborn S, Dooley J. 2010. *Pseudomonas aeruginosa* cystic fibrosis isolates of similar RAPD genotype exhibit diversity in biofilm forming ability in vitro. *BMC Microbiol.* 10:38. doi:10.1186/1471-2180-10-38
- Desai S, Sanghrajka K, Gajjar D. 2019. High adhesion and increased cell death contribute to strong biofilm formation in *Klebsiella pneumoniae*. *Pathogens.* 8:277. doi:10.3390/pathogens8040
- Djordjevic Z, Folic MM, Zivic Z, Markovic V, Jankovic SM. 2013. Nosocomial urinary tract infections caused by *Pseudomonas aeruginosa* and acinetobacter species: aensitivity to antibiotics and risk factors. *Am J Infect Control.* 41:1182–1187. doi:10.1016/j.ajic.2013.02.018
- Essar DW, Eberly L, Hadero A, Crawford IP. 1990. Identification and characterization of genes for a second anthranilate synthase in *Pseudomonas aeruginosa*: interchangeability of the two anthranilate synthases and evolutionary implications. *J Bacteriol.* 172:884–900. doi:10.1128/jb.172.2.884-900.1990
- Feneley RCL, Hopley IB, Wells PNT. 2015. Urinary catheters: history, current status, adverse events and research agenda. *J Med Eng Technol.* 39:459–470. doi:10.3109/03091902.2015.1085600
- Gomila A, Carratalà J, Eliakim-Raz N, Shaw E, Wiegand I, Vallejo-Torres L, Gorostiza A, Vigo JM, Morris S, Stoddart M, COMBACTE MAGNET WP5 RESCUING Study Group and Study Sites, et al. 2018. Risk factors and prognosis of complicated urinary tract infections caused by *Pseudomonas aeruginosa* in hospitalized patients: a retrospective multicenter cohort study. *Infect Drug Resist.* 11:2571–2581. doi:10.2147/IDR.S185753
- Harmsen M, Lappann M, Knochel S, Molin S. 2010. Role of extracellular DNA during biofilm formation by *Staphylococcus aureus*.

- monocytogenes. *Appl Environ Microbiol.* 76:2271–2279. doi:10.1128/AEM.02361-09
- Head NE, Yu H. 2004. Cross-sectional analysis of clinical and environmental isolates of *Pseudomonas aeruginosa*: biofilm formation, virulence, and genome diversity. *Infect Immun.* 72:133–144. doi:10.1128/IAI.72.1.133-144.2004
- Heidari H, Hadadi M, Sedigh Ebrahim-Saraie H, Mirzaei A, Tajji A, Hosseini SR, Motamedifar M. 2018. Characterization of virulence factors, antimicrobial resistance patterns and biofilm formation of *Pseudomonas aeruginosa* and *Staphylococcus* spp. strains isolated from corneal infection. *J Fr Ophthalmol.* 41:823–829. doi:10.1016/j.jfo.2018.01.012
- Hengge R. 2009. Principles of c-di-GMP signalling in bacteria. *Nat Rev Microbiol.* 7:263–273. doi:10.1038/nrmicro2109
- Horna G, Quezada K, Ramos S, Mosqueda N, Rubio M, Guerra H, Ruiz J. 2019. Specific type IV pili groups in clinical isolates of *Pseudomonas aeruginosa*. *Int Microbiol.* 22:131–141. doi:10.1007/s10123-018-00035-3
- Inclan YF, Huseby MJ, Engel JN. 2011. FimL regulates cAMP synthesis in *Pseudomonas aeruginosa*. *PLoS One.* 6:e15867. doi:10.1371/journal.pone.0015867
- Jarvis WR, Martone WJ. 1992. Predominant pathogens in hospital infections. *J Antimicrob Chemother.* 29:19–24. doi:10.1093/jac/29.suppl_A.19
- Jennings LK, Storek KM, Ledvina HE, Coulon C, Marmont LS, Sadovskaya I, Secor PR, Tseng BS, Scian M, Filloux A, et al. 2015. Pel is a cationic exopolysaccharide that cross-links extracellular DNA in the *Pseudomonas aeruginosa* biofilm matrix. *Proc Natl Acad Sci U S A.* 112:11353–11358. doi:10.1073/pnas.1503058112
- Jones CJ, Ryder CR, Mann EE, Wozniak DJ. 2013. AmrZ modulates *Pseudomonas aeruginosa* biofilm architecture by directly repressing transcription of the *psl* operon. *J Bacteriol.* 195:1637–1644. doi:10.1128/JB.02190-12
- Kamali E, Jamali A, Ardebili A, et al. Evaluation of antimicrobial resistance, biofilm forming potential, and the presence of biofilm-related genes among clinical isolates of *Pseudomonas aeruginosa*. *BMC Res Notes.* 2020;13:27. doi:10.1186/s13104-020-4890-z
- Knutson CA, Jeanes A. 1968. A new modification of the carbazole analysis: application to heteropolysaccharides. *Anal Biochem.* 24:470–481. doi:10.1016/0003-2697(68)90154-1
- Kragh KN, Alhede M, Kvich L, Bjarnsholt T. 2019. Into the well-A close look at the complex structures of a microtiter biofilm and the crystal violet assay. *Biofilm.* 1:100006. doi:10.1016/j.biofilm.2019.100006
- Lamas Ferreiro JL, Álvarez Otero J, González González L, Novoa Lamazares L, Arca Blanco A, Bermúdez Sanjurjo JR, Rodríguez Conde I, Fernández Soneira M, de la Fuente Aguado J. 2017. *Pseudomonas aeruginosa* urinary tract infections in hospitalized patients: mortality and prognostic factors. *PLoS ONE.* 12:e0178178–13. doi:10.1371/journal.pone.0178178
- Langendonk RF, Neill DR, Fothergill JL. 2021. The building blocks of antimicrobial resistance in *Pseudomonas aeruginosa*: implications for current resistance-breaking therapies. *Front Cell Infect Microbiol.* 11:665722–665759. doi:10.3389/fcimb.2021.665759
- Lara-Isla A, Medina-Polo J, Alonso-Isa M, Benítez-Sala R, Sopena-Sutil R, Justo-Quintas J, Gil-Moradillo J, González-Padilla DA, García-Rojo E, Passas-Martínez JB, et al. 2017. Urinary infections in patients with catheters in the upper urinary tract: microbiological study. *Urol Int.* 98:442–448. doi:10.1159/000467398
- Lee KH, Park SJ, Choi SJ, Uh Y, Park JY, Han KH. 2017. The influence of urinary catheter materials on forming biofilms of microorganisms. *J Bacteriol Virol.* 47:32–40. doi:10.4167/jbv.2017.47.1.32
- Lister PD, Wolter DJ, Hanson ND. 2009. Antibacterial-resistant *Pseudomonas aeruginosa*: clinical impact and complex regulation of chromosomally encoded resistance mechanisms. *Clin Microbiol Rev.* 22:582–610. doi:10.1128/CMR.00040-09
- Luther MK, Parente DM, Caffrey AR, Daffinee KE, Lopes VV, Martin ET, Laplante KL. 2018. Clinical and genetic risk factors for biofilm-forming *Staphylococcus aureus*. *Antimicrob Agents Chemother.* 62:e02252–e02317 doi:10.1128/AAC.02252-17
- Ma L, Conover M, Lu H, Parsek MR, Bayles K, Wozniak DJ. 2009. Assembly and development of the *Pseudomonas aeruginosa* biofilm matrix. *PLoS Pathog.* 5:e1000354. doi:10.1371/journal.ppat.1000354
- Madsen JS, Lin YC, Squyres GR, Price-Whelan A, Torio A de S, Song A, Cornell WC, Sørensen SJ, Xavier JB, Dietrich LEP. 2015. Facultative control of matrix production optimizes competitive fitness in *Pseudomonas aeruginosa* PA14 biofilm models. *Appl Environ Microbiol.* 81:8414–8426. doi:10.1128/AEM.02628-15
- Mattick JS. 2002. Type IV pili and twitching motility. *Annu Rev Microbiol.* 56:289–314. doi:10.1146/annurev.micro.56.012302.160938
- Mirzahosseini H, Haddadi Fishani M, Morshedi K. Meta-Analysis of Biofilm Formation, Antibiotic Resistance Pattern, and Biofilm-Related Genes in *Pseudomonas aeruginosa* Isolated from Clinical Samples. *Microbial Drug Resistance.* 2020;26. doi:10.1089/mdr.2019.0274
- Kumari M, Khurana S, Bhardwaj N, Malhotra R, Purva M. 2019. Pathogen burden & associated antibiogram of *Pseudomonas* spp. in a tertiary care hospital of India. *Indian J Med Res.* 149:295–298. doi:10.4103/ijmr.IJMR_14_18
- Mulcahy LR, Isabella VM, Lewis K. 2014. *Pseudomonas aeruginosa* biofilms in disease. *Microb Ecol.* 68:1–12. doi:10.1007/s00248-013-0297-x
- Nolan LM, McCaughey LC, Merjane J, Turnbull L, Whitchurch CB. 2020. ChpC controls twitching motility-mediated expansion of *Pseudomonas aeruginosa* biofilms in response to serum albumin, mucin and oligopeptides. *Microbiology (Reading).* 166:669–678. doi:10.1099/mic.0.000911
- O'Toole GA. 2011. Microtiter dish biofilm formation assay. *J Vis Exp.* 30;(47):2437. doi:10.3791/2437
- O'Toole GA, Kolter R. 1998. Flagellar and twitching motility are necessary for *Pseudomonas aeruginosa* biofilm development. *Mol Microbiol.* 30:295–304. doi:10.1046/j.1365-2958.1998.01062.x
- Pinzon NM, Ju L. 2009. Analysis of rhamnolipid biosurfactants by methylene blue complexation. *Appl Microbiol Biotechnol.* 82:975–981. doi:10.1007/s00253-009-1896-9

- Pratt LA, Kolter R. 1998. Genetic analysis of *Escherichia coli* biofilm formation: roles of flagella, motility, chemotaxis and type I pili. *Mol Microbiol.* 30:285–293. doi:10.1046/j.1365-2958.1998.01061.x
- Reichhardt C, Jacobs HM, Matwchuk M, Wong C, Wozniak DJ, Parsek MR. 2020. The Versatile *Pseudomonas aeruginosa* biofilm matrix protein CdrA promotes aggregation through different extracellular exopolysaccharide interactions. *J Bacteriol.* 202:1–9. doi:10.1128/JB.00216-20
- Reichhardt C, Wong C, da Silva DP, Wozniak DJ, Parsek MR. 2018. CDRA interactions within the *Pseudomonas aeruginosa* biofilm matrix safeguard it from proteolysis and promote cellular packing. *MBio.* 9:1–12. doi:10.1128/mBio.01376-18
- Römling U, Galperin MY, Gomelsky M. 2013. Cyclic di-GMP: the first 25 years of a universal bacterial second messenger. *Microbiol Mol Biol Rev.* 77:1–52. doi:10.1128/mbr.00043-12
- Ryder C, Byrd M, Wozniak DJ. 2007. Role of polysaccharides in *Pseudomonas aeruginosa* biofilm development. *Curr Opin Microbiol.* 10:644–648. doi:10.1016/j.mib.2007.09.010
- Sarkar S. 2020. Release mechanisms and molecular interactions of *Pseudomonas aeruginosa* extracellular DNA. *Appl Microbiol Biotechnol.* 104:6549–6564. doi:10.1007/s00253-020-10687-9
- Saxena S, Banerjee G, Garg R, Singh M. Comparative Study of Biofilm Formation in *Pseudomonas aeruginosa* Isolates from Patients of Lower Respiratory Tract Infection. *J Clin Diagn Res.* 2014;8(5):DC09–11. doi:10.7860/JCDR/2014/7808.4330
- Shigemura K, Arakawa S, Sakai Y, Kinoshita S, Tanaka K, Fujisawa M. 2006. Complicated urinary tract infection caused by *Pseudomonas aeruginosa* in a single institution (1999–2003). *Int J Urol.* 13:538–542. doi:10.1111/j.1442-2042.2006.01359.x
- Stepanović S, Ćirković I, Ranin L, Švabić-Vlahović M. 2004. Biofilm formation by *Salmonella* spp. and *Listeria monocytogenes* on plastic surface. *Lett Appl Microbiol.* 38:428–432. doi:10.1111/j.1472-765X.2004.01513.x
- Suriyanarayanan T, Qingsong L, Kwang LT, Mun LY, Truong T, Seneviratne CJ. 2018. Quantitative proteomics of strong and weak biofilm formers of enterococcus faecalis reveals novel regulators of biofilm formation. *Mol Cell Proteomics.* 17:643–654. doi:10.1074/mcp.RA117.000461
- Tellis RC, Mososabba MS, Roche RA. 2017. Correlation between biofilm formation and antibiotic resistance in uropathogenic *Pseudomonas aeruginosa* causing catheter associated urinary tract infections. *Eur J Pharm Med Res.* 4:248–252.
- Tetz GV, Artemenko NK, Tetz VV. 2009. Effect of DNase and antibiotics on biofilm characteristics. *Antimicrob Agents Chemother.* 53:1204–1209. doi:10.1128/AAC.00471-08
- Thi MTT, Wibowo D, Rehm BHA. 2020. *Pseudomonas aeruginosa* biofilms. *IJMS.* 21:8625–8671. doi:10.3390/ijms21228671
- Thibeaux R, Kainiu M, Goarant C. 2020. Biofilm formation and quantification using the 96-microtiter plate. *Methods Mol Biol.* 2134:207–214. doi:10.1007/978-1-0716-0459-5_19
- Valentini M, Filloux A. 2016. Biofilms and Cyclic di-GMP (c-di-GMP) signaling: lessons from *Pseudomonas aeruginosa* and other bacteria. *J Biol Chem.* 291:12547–12555. doi:10.1074/jbc.R115.711507
- Vipin C, Mujeeburahiman M, Arun AB, Ashwini P, Mangesh SV, Rekha PD. 2019. Adaptation and diversification in virulence factors among urinary catheter-associated *Pseudomonas aeruginosa* isolates. *J Appl Microbiol.* 126:641–650. doi:10.1111/jam.14143
- Webb JS, Thompson LS, James S, Charlton T, Tolker-Nielsen T, Koch B, Givskov M, Kjelleberg S. 2003. Cell death in *Pseudomonas aeruginosa* biofilm development. *J Bacteriol.* 185:4585–4592. doi:10.1128/JB.185.15.4585-4592.2003
- Wu J, Xi C. 2009. Evaluation of different methods for extracting extracellular DNA from the biofilm matrix. *Appl Environ Microbiol.* 75:5390–5395. doi:10.1128/AEM.00400-09
- Xu ZG, Gao Y, He JG, Xu WF, Jiang M, Jin HS. 2015. Effects of azithromycin on *Pseudomonas aeruginosa* isolates from catheter-associated urinary tract infection. *Exp Ther Med.* 9:569–572. doi:10.3892/etm.2014.2120
- Zhang W, Sun J, Ding W, Lin J, Tian R, Lu L, Liu X, Shen X, Qian PY. 2015. Extracellular matrix-associated proteins form an integral and dynamic system during *Pseudomonas aeruginosa* biofilm development. *Front Cell Infect Microbiol.* 5:10–40. doi:10.3389/fcimb.2015.00040
- Zheng S, Bawazir M, Dhall A, Kim HE, He L, Heo J, Hwang G. 2021. Implication of surface properties, bacterial motility, and hydrodynamic conditions on bacterial surface sensing and their initial adhesion. *Front Bioeng Biotechnol.* 9:643722–643722. doi:10.3389/fbioe.2021.643722.

Appendices

AU	Artificial Urine
CAUTI	Catheter Associated Urinary Tract infections
CLSM	Confocal Laser Scanning Electron Microscope
CV	Crystal Violet
E-SEM	Environmental- Scanning Electron Microscope
eDNA	extracellular DNA
LB	Luria Broth
NA	Natural Urine
TSB	Tryptone Soya Broth
T4P	Type 4 pili
OD	Optical density
ODc	Cutt-off OD value
UTI	Urinary Tract Infection



OPEN Pseudomonas aeruginosa persister cell formation upon antibiotic exposure in planktonic and biofilm state

Hiral Patel, Hasmatbanu Buchad & Devarshi Gajjar

Persister cell (PC) is dormant, tolerant to antibiotics, and a transient reversible phenotype. These phenotypes are observed in *P. aeruginosa* and cause bacterial chronic infection as well as recurrence of biofilm-mediated infection. PC formation requires stringent response and toxin-antitoxin (TA) modules. This study shows the *P. aeruginosa* PC formation in planktonic and biofilm stages on ceftazidime, gentamicin, and ciprofloxacin treatments. The PC formation was studied using persister assay, flow cytometry using Redox Sensor Green, fluorescence as well as Confocal Laser Scanning Microscopy, and gene expression of stringent response and TA genes. In the planktonic stage, ceftazidime showed a high survival fraction, high redox activity, and elongation of cells was observed followed by ciprofloxacin and gentamicin treatment having redox activity and rod-shaped cells. The gene expression of stringent response and TA genes were upregulated on gentamicin followed by ceftazidime treatment and varied among the isolates. In the biofilm stage, gentamicin and ciprofloxacin showed the biphasic killing pattern, redox activity, gene expression level of stringent response and TA varied across the isolates. Ceftazidime treatment showed higher persister cells in planktonic growth while all three antibiotics were able to induce persister cell formation in the biofilm stage.

Persister cell (PC) is a non-growing and metabolically inactive cell, which lacks transcription, translation, and proton motive force. PC formation is reported to occur stochastically or under various conditions such as (i) upon antibiotic treatment (ii) nutrient deprivation and (iii) biofilms^{1–3}. PC are responsible for chronic bacterial infections and relapse of biofilm infections^{4–6}. Within the biofilm matrix, the PC escape from the attack of the host immune system and other harsh environmental conditions⁴. *Pseudomonas aeruginosa* (*P. aeruginosa*) is an opportunistic pathogen frequently causing chronic airway infections in patients with cystic fibrosis (CF), urinary tract infections (UTIs) and ventilator-associated pneumonia. It is also involved in persistent infections and biofilm-related infections^{7,8}. The majority of in vitro data on PC has been focused on the exponential and stationary phase of *Escherichia coli* (*E. coli*).

In recent years studies have shown elements required for stringent response and persistence are ppGpp alarmone, SpoT, RelA, DksA, Lon, and Toxin-Antitoxin (TA) modules, and the regulatory role of these elements is well characterized in *P. aeruginosa* (PAO1)⁹. Antibiotics; ciprofloxacin, cefepime, colistin, and amikacin were shown to upregulate *relA* gene expression, apart from induction of *relA*, persister formation might also occur from different mechanisms with different antibiotics in the planktonic stage¹⁰. In *E. coli* the Lon protease degrades the antitoxin which leads to the accumulation of toxins leading to PC formation¹¹. However, in *P. aeruginosa* the Lon protease activity is induced by aminoglycosides and necessary for virulence, motility, and biofilm formation¹². In *P. aeruginosa*, biofilms increase the PC formation^{13,14}, and the association of TA systems in persister formation is documented in type strain PAO1. Among which ParD/ParE¹⁵, HicA/HicB¹⁶, RelE/RelB¹⁷, and HigB/HigA¹⁸ TA systems are identified in *P. aeruginosa*. The well-studied type II TA system HigB/HigA influences swarming motility, biofilm formation, and virulence factors such as pyochelin and pyocyanin^{18,19}. HigB reduces the biofilm formation through (i) reducing the intracellular c-di-GMP level through activation of c-di-GMP hydrolysis genes, which (ii) upregulates the expression of the type 3 secretion system (T3SS)¹⁹. Additionally, subsequent exposure to ciprofloxacin antibiotic results in PC formation via activation of RelA/

Department of Microbiology and Biotechnology Centre, Faculty of Science, The Maharaja Sayajirao University of Baroda, Vadodara, Gujarat 390002, India. email: devarshi.gajjar-microbio@msubaroda.ac.in

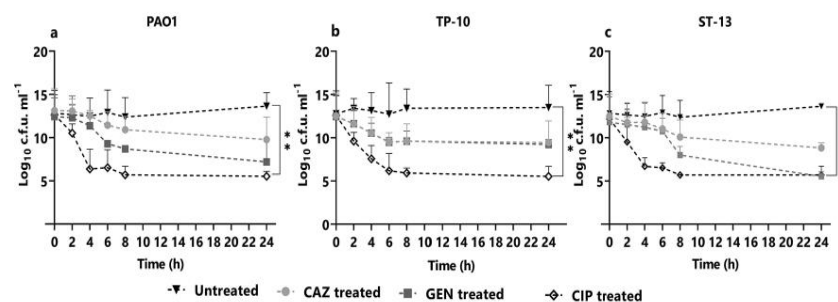


Figure 1. Planktonic time-kill curve assay. The planktonic stage of *P. aeruginosa*: (a) POA1, (b) TP-10, and (c) ST-13 were grown in LB and treated with CAZ, GEN, CIP at 5× MIC. At t = 2, 4, 6, 8, and 24 h cells were plated for the viable count. Without treatment was used as a control. CAZ: ceftazidime; GEN: gentamicin, and CIP: ciprofloxacin. Statistical analysis was performed using one-way ANOVA, which was * $P < 0.05$, ** $P < 0.01$.

SpoT and HigB/HigA TA system in biofilm²⁰. Similarly, upon exposure to DNA gyrase inhibitor antibiotics the TA system ParD/ParE gets activated¹⁵.

The TA system and Lon protease have not been studied at supra-MIC concentration of antibiotics, and their significant role in biofilm tolerance as well as in the planktonic stage remains to be elucidated. In this study, we enumerate PC formation in the planktonic and biofilm stage with exposure to three different antibiotics (ceftazidime, gentamicin, and ciprofloxacin) in *P. aeruginosa*.

Results

Antimicrobial susceptibility of *P. aeruginosa* isolates. Supplementary Table S1 shows the MIC values of the *P. aeruginosa* clinical isolates: TP-10, ST-13, and PAO1 (as reference strain) ($n = 3$) for the respective antibiotics (ceftazidime, gentamicin, and ciprofloxacin). As per CLSI guidelines, PAO1 and ST-13 isolates were resistant to ciprofloxacin, while susceptible to ceftazidime and gentamicin antibiotics. The TP-10 isolate was susceptible to all antibiotics.

Persister cell formation in the planktonic stage. *P. aeruginosa* isolates (PAO1, TP10, and ST13) were studied for PC formation using three bactericidal antibiotics: ceftazidime (Cephalosporin), gentamicin (aminoglycoside), and ciprofloxacin (fluoroquinolone) at 5X MIC. Figure 1 shows the time-kill curve assay for PAO1, TP10, and ST13 isolates using three antibiotics at 5X MIC concentration at indicated time points for 24 h. The biphasic killing pattern, which is a hallmark for PC, varied across the isolates. In the PAO1 strain, ceftazidime showed the least log reduction and formed a considerably higher cell survival fraction ($9 \log_{10}$ cfu/ml) (Fig. 1a). Gentamicin treatment formed $8 \log_{10}$ cfu/ml, whereas ciprofloxacin treatment resulted in $6 \log_{10}$ cfu/ml (Fig. 1a). Further in the TP-10 isolate, gentamicin and ceftazidime treatment formed a $9 \log_{10}$ cfu/ml survival fraction (Fig. 1b) and ciprofloxacin treatment resulted in the cell survival fraction of $6 \log_{10}$ cfu/ml. In the ST-13 isolate, on ceftazidime treatment the survival fraction was $9\text{--}10 \log_{10}$ cfu/ml (Fig. 1c). On gentamicin and ciprofloxacin treatment the range of survival fraction was $5\text{--}6 \log_{10}$ cfu/ml (Fig. 1c). The maximum log reduction was observed by ciprofloxacin treatment and least persister cells were formed compared to other antibiotic treatments.

Cellular redox activity in the planktonic stage. The cellular redox activity in the planktonic stage of isolates PAO1, TP-10, and ST-13 was done using RSG and PI staining. The RSG dye can easily penetrate bacteria and yield green fluorescence when reduced by bacterial reductases which can be correlated with cellular metabolic activities^{21,22}. Figure 2a–c shows the flow cytometry of PAO1, TP-10, and ST-13 isolates with and without antibiotic treatments after 4 h. In PAO1 isolate, ceftazidime treatment leads to an increase in redox activity compared to untreated (Fig. 2a). Whereas, on gentamicin and ciprofloxacin treatment there was a decrease in redox activity (Fig. 2a). When compared to an untreated TP-10, ceftazidime treatment increased redox activity, followed by ciprofloxacin and gentamicin treatment (Fig. 2b). Ceftazidime treatment has increased redox activity in the ST-13 compared to untreated, followed by gentamicin and ciprofloxacin (Fig. 2c). Figure 2d–f shows the flow cytometry analysis of the number of RSG positive cells of antibiotic-treated and untreated. In PAO1 there is a significant increase in redox activity on ceftazidime treated compared to untreated. While redox activity was decreased on gentamicin and ciprofloxacin (Fig. 2d). In the TP-10, there is a significant difference in RSG fluorescence after ceftazidime and ciprofloxacin treatment compared to untreated cells (Fig. 2e). While there was no significant difference observed in the ST-13 isolate (Fig. 2f).

Fluorescent microscopy of the planktonic stage. Figure 3 shows the fluorescence microscopy images of PC formation after 4 h of antibiotic treatment at 5X MIC. In PAO1 isolate, ceftazidime treatments lead to the filamentous form of cells, while gentamicin and ciprofloxacin had rod-shaped cells (Fig. 3b–d). In TP-10 isolate, on ceftazidime treatment, elongated cells were observed as PAO1, while on gentamicin and ciprofloxacin treatment rod-shaped cells were observed (Fig. 3f–h). Apart from this, the high redox-active cells were present

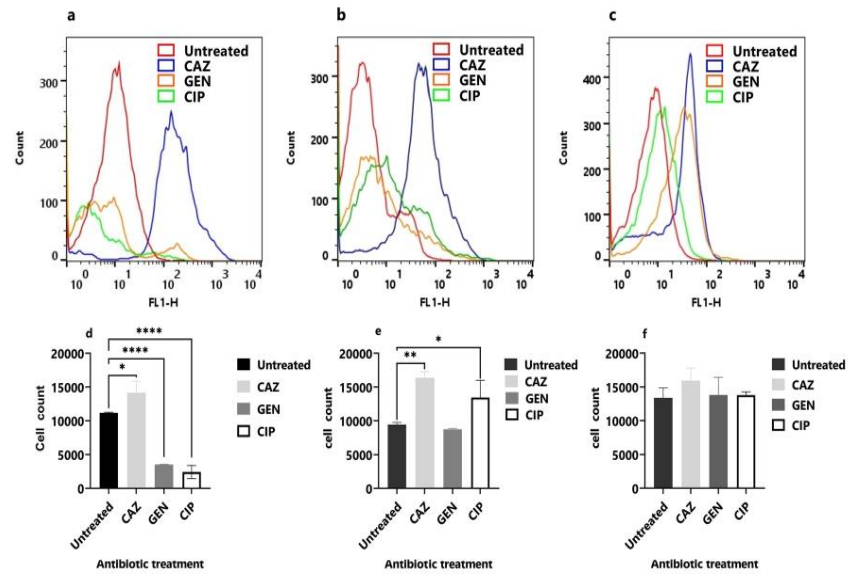


Figure 2. Cellular redox activity of planktonic cells. The flow cytometry of (a) PAO1, (b) TP-10 and (c) ST-13 isolate was done using RSG staining after 4 h of antibiotics treatment (CAZ, GEN, and CIP). Untreated was used as a control. (d–f) The quantitative data of RSG-positive cells (in PAO1, TP-10 and ST-13) using flow cytometry analysis after treatment with respective antibiotics were compared to the untreated control. CAZ: ceftazidime, GEN: gentamicin, and CIP: ciprofloxacin. The corresponding data represent the mean \pm standard deviation. The experiment was performed in three biological triplicates for each strain. Statistical analysis was performed using a one-way ANOVA, which was * $P < 0.05$, and ** $P < 0.01$, *** $P < 0.001$, **** $P < 0.0001$.

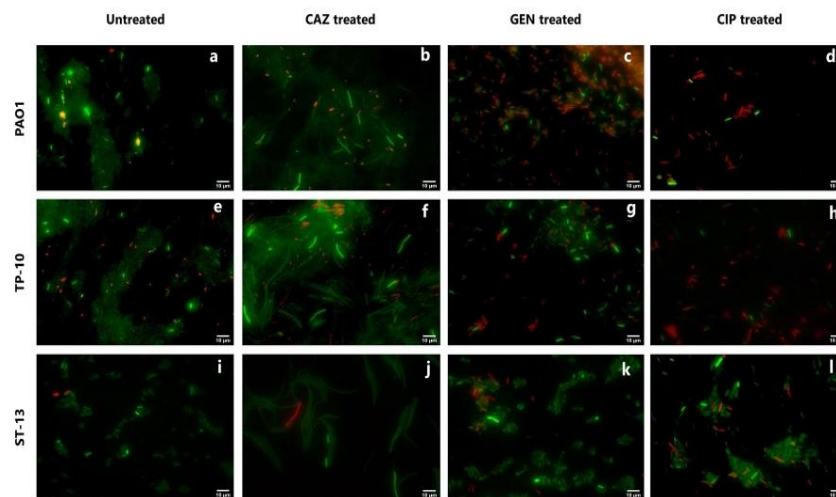


Figure 3. Fluorescence Microscopy of PCs in the planktonic stage. The representative images of PAO1, TP-10, and ST-13 isolates, after 4 h of (a,e,i) without antibiotic treatment and with (b,f,j) CAZ (c,g,k) GEN (d,h,l) CIP antibiotic treatments, which were grown in LB. Before staining the cells were washed to remove antibiotics and stained with RSG and PI dyes. (a,e,i) Untreated cells were used as control. Cellular redox activity was measured by RSG staining. CAZ: ceftazidime, GEN: gentamicin, and CIP: ciprofloxacin. Images were analysed using Fiji software.

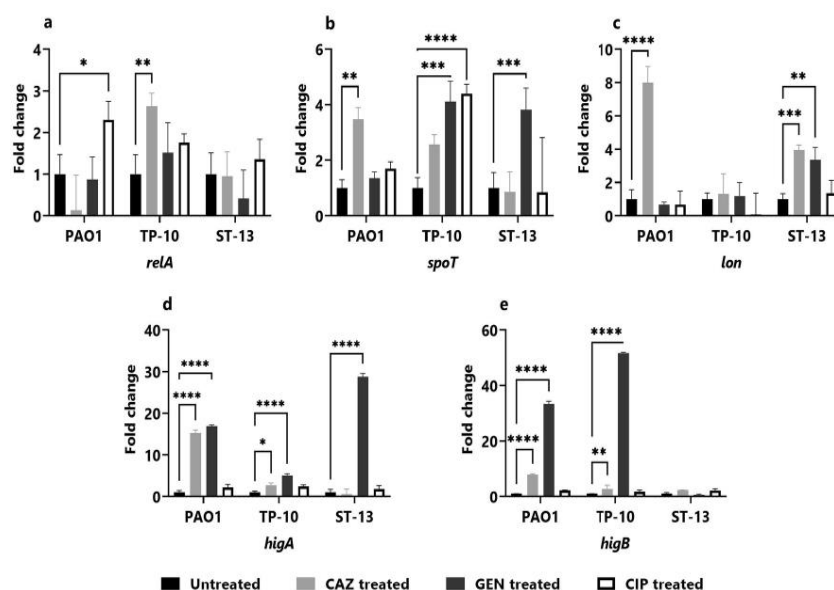


Figure 4. Gene expression studies in the planktonic stage. The gene expression of stringent response genes: (a) *relA*, (b) *spoT*, and (c) *lon* as well as toxin-antitoxin genes: (d) *higA* and (e) *higB* was studied in PAO1, TP-10 and ST-13 isolate after 4 h of antibiotic (CAZ, GEN, and CIP) treatment. The gene expression was normalized with untreated control. CAZ: ceftazidime, GEN: gentamicin, and CIP: ciprofloxacin. The experiment was performed in three biological experiments for each strain. Data represent the mean \pm standard deviation of fold change. The Statistical analysis was performed using the two-way ANOVA, which was * $P < 0.05$, ** $P < 0.01$, *** $P < 0.001$, and **** $P < 0.0001$.

on ceftazidime and gentamicin treatments in the PAO1 (Fig. 3b,c), and TP-10 (Fig. 3f,g). On the ciprofloxacin treatment, there were fewer high redox-active cells and more number of cells were killed (Fig. 3d,h). While in ST-13, the ceftazidime antibiotic leads to elongation of cells with high redox activity (Fig. 3j). The gentamicin and ciprofloxacin treatment had rod shape cells, where the number of high redox-active cells was less in number (Fig. 3k,l).

Gene expression in the planktonic stage. To gain a better understanding of the mechanism behind the *P. aeruginosa* (PAO1, TP-10, and ST-13) persistence in the planktonic stage upon ceftazidime, gentamicin, and ciprofloxacin treatment, the gene expression was studied for antibiotic tolerance: stringent response genes (*relA*, *spoT*, and *lon*) and the toxin-antitoxin genes (*higA* and *higB*) involved in PC formation.

Figure 4 depicts the variation of the gene expression across isolates (PAO1, TP-10, and ST-13) in the planktonic stage, with antibiotic treatments showing upregulation of genes as compared to untreated. The *relA* gene expression was 2.30 ± 0.44 -fold higher on ciprofloxacin treatment in PAO1, and 2.63 ± 0.32 -fold higher on ceftazidime treatment in TP-10 (Fig. 4a). Further, *spoT* gene expression was 3.44 ± 0.43 -fold upregulated on ceftazidime treatment in PAO1 and 4.11 ± 0.72 and 4.40 ± 0.34 -fold higher on gentamicin and ciprofloxacin treatment, respectively in TP-10 (Fig. 4b). While in ST-13 upregulation of *spoT* gene was 3.81 ± 0.78 -fold higher on gentamicin treatment (Fig. 4b). The *lon* gene expression was increased by 7.99 ± 0.96 -fold on ceftazidime treatment in PAO1, and 3.94 ± 0.30 and 3.36 ± 0.074 -fold increase in response to ceftazidime and gentamicin treatment, in ST-13 (Fig. 4c). Additionally, the expression of *higA* gene was significantly upregulated by 15.26 ± 0.70 and 16.88 ± 0.30 -fold on ceftazidime and gentamicin treatment, respectively, in PAO1 (Fig. 4d). Also, the *higA* gene was a 2.72 ± 0.52 and 5.05 ± 0.42 -fold increase on ceftazidime and gentamicin treatment in TP-10 and 28.77 ± 0.80 -fold high on gentamicin treatment in ST-13 (Fig. 4d). The expression of *higB* gene was 7.90 ± 0.33 and 33.33 ± 1.02 -fold upregulated on ceftazidime and gentamicin treatment in PAO1, while 2.74 ± 1.3 and 51.63 ± 0.35 upregulated on ceftazidime and gentamicin in TP-10 (Fig. 4e).

Persister cell formation in the biofilm stage. Biofilm formation was analyzed for all three isolates using crystal violet assay, in which PAO1 and ST-13 were found to be strong biofilm producers and TP-10 was a weak biofilm producer (Supplementary Fig. S1). To analyze the PC formation in biofilm conditions, a biofilm time-kill curve experiment was performed for PAO1, TP-10, and ST-13 isolates against three antibiotics as shown in Fig. 5a. The mean inoculum varied between isolates, ranging from 5–6 \log_{10} cfu/ml for TP-10 and ST-13 to 11–12 \log_{10} cfu/ml for PAO1. After 24 h of ceftazidime treatment, all isolates were regrown to the same cfu/ml as the growth control (Fig. 5a–c). In all three isolates, the biphasic kill curve was observed for gentamicin

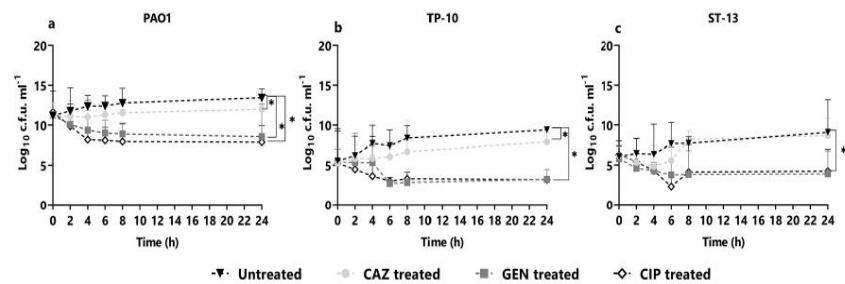


Figure 5. Biofilm time-kill curve assay. The biofilm formed for 24 h of (a) PAO1, (b) TP-10, and (c) ST-13, grown in MHB, were treated with CAZ, GEN, CIP at 5× MIC concentration. At indicated time points of t=2, 4, 6, 8, and 24 h cells were plated for the viable count. Without treatment was used as a control. CAZ: ceftazidime, GEN: gentamicin, and CIP: ciprofloxacin. Statistical analysis was performed using one-way ANOVA, which was * $P < 0.05$, ** $P < 0.01$.

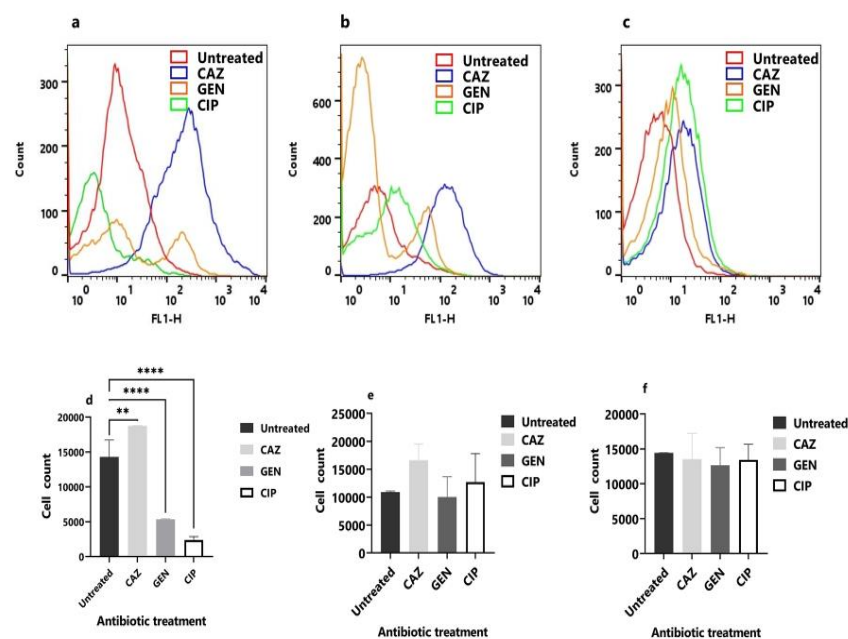


Figure 6. Cellular redox activity in the biofilm stage. The flow cytometry of (a) PAO1 (b) TP-10 and (c) ST-13 biofilms was done using RSG and PI staining after 4 h of antibiotics treatment (CAZ, GEN, and CIP). Untreated was used as a control. (d–f) The quantitative data of RSG-positive cells (in PAO1, TP-10 and ST-13) using flow cytometry analysis after treatment with respective antibiotics were compared to the untreated control. CAZ: ceftazidime, GEN: gentamicin, and CIP: ciprofloxacin. The corresponding data represent the mean \pm standard deviation. The experiment was performed in three biological triplicates for each strain. Statistical analysis was performed using a one-way ANOVA, which were * $P < 0.05$, and ** $P < 0.01$, *** $P < 0.001$, and **** $P < 0.0001$.

and ciprofloxacin antibiotic treatment (Fig. 5a–c). The biphasic curve showed an initial log decrease in PAO1 biofilm after treatment with gentamicin and ciprofloxacin, followed by 8–9 \log_{10} cfu/ml and 8 \log_{10} cfu/ml cell surviving fractions. In TP-10 biofilm, approximately 2–3 \log_{10} cfu/ml cell survival fractions were formed in biphasic kill curves on gentamicin and ciprofloxacin treatment. In addition to gentamicin and ciprofloxacin treatment, 3–4 \log_{10} cfu/ml cell survival fractions were observed in ST-13 biofilm.

Cellular redox activity in the biofilm stage. The cellular redox activity in the biofilm stage after 4 h of antibiotic treatments (Ceftazidime, gentamicin, and ciprofloxacin) was studied using flow cytometry (Fig. 6). In PAO1, ceftazidime treatment leads to an increase in redox activity compared to control (Fig. 6a). Whereas, there was no increase in redox-active cells on gentamicin and ciprofloxacin treatments (Fig. 6a). In the TP-10 biofilm, the ceftazidime treatment showed high redox-active cells followed by gentamicin and ciprofloxacin

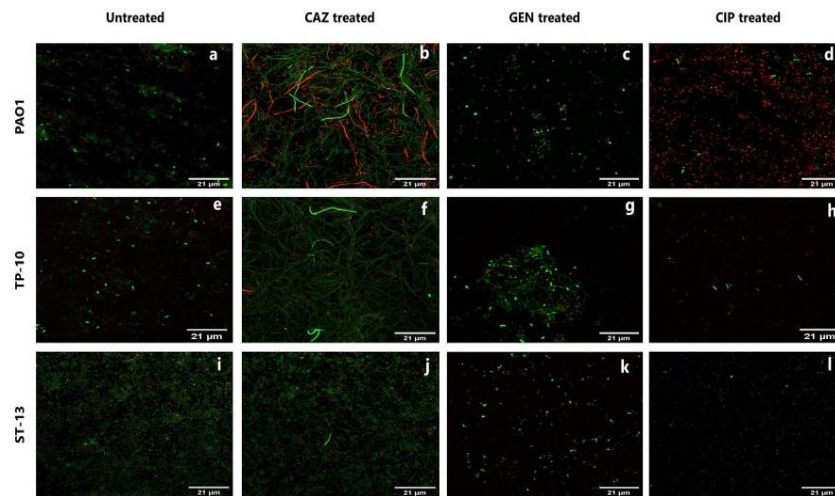


Figure 7. CLSM of PC in the biofilm stage. The representative images of PAO1, TP-10, and ST-13 biofilm, grown in MHB, after 4 h of (a,e,i) without antibiotic treated and antibiotic treatment with (b,f,j) CAZ, (c,g,k) GEN, and (d,h,l) CIP. Biofilm was rinsed with 0.85% NaCl to remove any residue of antibiotics and staining was done using RSG and PI dyes. CAZ: ceftazidime, GEN: gentamicin, and CIP: ciprofloxacin. Images were analysed using Fiji software.

compared to untreated (Fig. 6b). While in ST-13 biofilm, high redox-active cells were observed on ceftazidime treatment followed by ciprofloxacin and gentamicin (Fig. 6c). Figure 6d–f depicts flow cytometry analysis of RSG positive cells after antibiotic treatments. In PAO1 biofilm, ceftazidime treatment resulted in a high number of redox-active cells than untreated control (Fig. 6d). While a decrease in redox-active cells was observed on gentamicin and ciprofloxacin treatments (Fig. 6d). In TP-10 and ST-13 biofilm, no significant difference in redox activity was observed compared to untreated control (Fig. 6e,f).

CLSM microscopy of the biofilm stage. The cellular redox activity within the biofilm formed by PAO1, TP-10, and ST-13 after 4 h of treatment with antibiotics were visualized by CLSM using RSG and PI staining (Fig. 7). Biofilms formed by three isolates showed varying thickness. In PAO1 biofilm, treated had high redox-active cells compared to untreated one (Fig. 7a–d). Ceftazidime treatment had elongated cells; however, the high redox-active cells were observed less (Fig. 7b). On gentamicin and ciprofloxacin treatment rod-shaped high redox-active cells were observed as well as disrupted biofilm and dead cells were high in number in ciprofloxacin treated PAO1 biofilm (Fig. 7c,d). On ceftazidime treatment, elongation of cells observed with few redox-active cells was observed in TP-10 biofilm compared to the untreated (Fig. 7e,f). On gentamicin treatment, rod-shaped high redox-active cells were observed in TP-10 biofilm (Fig. 7g). Whereas on ciprofloxacin treatment TP-10 biofilm was disrupted and fewer higher redox active cells were observed (Fig. 7h). ST-13 isolate had thick biofilm in untreated, ceftazidime treatment had very less elongation of cells with a smaller number of redox-active cells (Fig. 7i,j). On gentamicin treatment had rod-shaped high redox-active cells and biofilm was disrupted in ST-13 biofilm (Fig. 7k). While ciprofloxacin treatment had less number of cells compared to untreated and biofilm was disrupted having fewer redox-active cells (Fig. 7l).

Gene expression in biofilm stage. After 4 h of antibiotic treatment, the gene expression of stringent response genes (*relA*, *spoT*, and *lon*), and the toxin-antitoxin genes (*higA* and *higB*) involved in PCs formation was examined, and compared with untreated (Fig. 8). The expression of *relA* gene was elevated by 3.78 ± 0.50 -fold and 4.40 ± 3.50 -fold on ceftazidime treatment, in PAO1 and TP-10 respectively (Fig. 8a). The expression of *relA* gene was upregulated by 2.94 ± 0.25 and 3.50 ± 0.52 -fold on gentamicin and ciprofloxacin treatment in ST-13 (Fig. 8a). The *spoT* gene was increased by $3.61, \pm 0.47$ -fold on ceftazidime treatment in TP-10, and 2.31 ± 0.311 and 2.60 ± 0.68 -fold increased on gentamicin and ceftazidime treatment in ST-13 (Fig. 8b). The *lon* gene was 9.45 ± 0.42 and 5.01 ± 0.02 -fold higher on ceftazidime treatment in PAO1 and TP-10, respectively (Fig. 8c). Further, *higA* gene was upregulated by 2.24 ± 0.12 -fold on ceftazidime treatment in TP-10 and 1.91 ± 0.68 , 3.50 ± 0.34 , and 2.24 ± 0.48 -fold in all three-antibiotic treatment in ST-13 (Fig. 8d). Additionally, the expression of *higB* gene was 2.50 ± 1.05 , and 2.09 ± 0.68 -fold high on ceftazidime and ciprofloxacin treatment in ST-13 (Fig. 8e).

Discussion

The persistence phenomenon is a type of phenotypic switch that allows the subpopulation of bacteria to survive under antibiotic exposure and is associated with recurrent infections and antibiotic treatment failure. PC formation is a complex survival strategy and depends upon various factors that include growth phase, expression

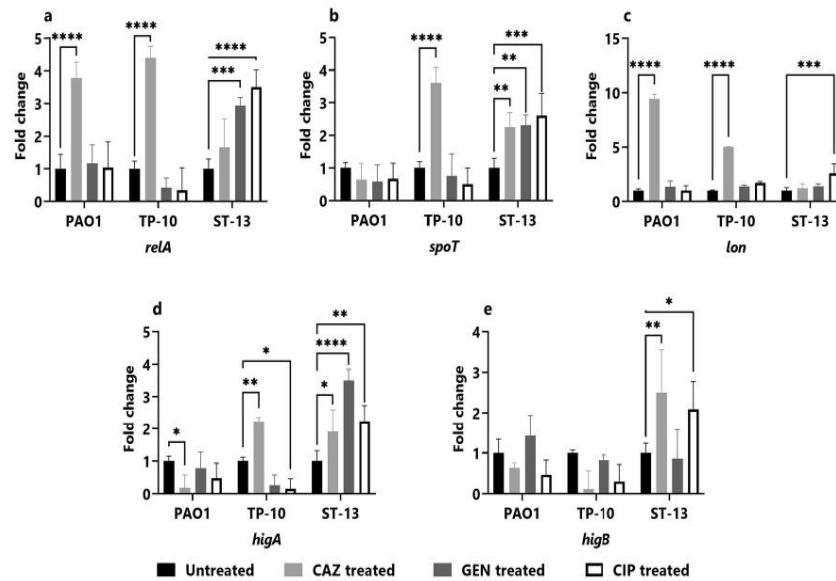


Figure 8. Gene expression studies in the biofilm stage. The gene expression of stringent response genes: (a) *relA*, (b) *spoT*, and (c) *lon* as well as toxin-antitoxin genes: (d) *higA* and (e) *higB* was studied in PAO1, TP-10, and ST-13 biofilms after 4 h of antibiotic (CAZ, GEN, and CIP) treatment. Prior to it, the biofilm was formed for 24 h in six well plates. The gene expression was normalized to the untreated control. CAZ: ceftazidime, GEN: gentamicin, CIP: ciprofloxacin. The three biological experiments were performed for each strain. The corresponding data represents the mean \pm standard deviation of fold change. The statistical analysis was performed using the two-way ANOVA, which was * $P < 0.05$, ** $P < 0.01$, *** $P < 0.001$, and **** $P < 0.0001$.

of stringent response genes, toxin-antitoxin systems, quorum sensing, and SOS response¹³. Many studies have documented PC formation upon antibiotic exposure with respect to the type strains of *P. aeruginosa*; PAO1 and PA14^{14,17,20}. The present study highlights the PC formation in response to exposure of three antibiotics belonging to different classes: ceftazidime, gentamicin, and ciprofloxacin in PAO1, TP-10, and ST-13 strains under two physiological conditions (planktonic and biofilm stage). The effect of three antibiotics that lead to PC formation was analyzed by measuring the redox activity and expression of stringent response as well as toxin-antitoxin genes in planktonic and biofilm conditions.

In the planktonic stage, ceftazidime showed a biphasic kill-curve in all isolates; showing the presence of PCs. However, the effect of gentamicin and ciprofloxacin was diverse across the isolates (Fig. 1). Further, the presence of PCs was confirmed using RSG staining where a difference in cellular redox activity was observed between the strains, and high redox activity was seen under ceftazidime treatment followed by ciprofloxacin and gentamicin. The difference in redox activity observed among isolates is due to the difference in survival fractions observed in cfu/ml data. A similar study showed more survival fraction in β -lactam (carbenicillin) treatment compared to fluoroquinolone (ofloxacin) and an aminoglycoside (tobramycin)²³. Reduced survival rate upon ciprofloxacin treatment that kills non-growing cells also showed variability across the clinical isolates of *P. aeruginosa*^{10,24}. In this study, microscopy of antibiotic treated planktonic cells showed filamentous PCs with high redox activity upon ceftazidime treatment (Fig. 3). The ceftazidime treatment causes filamentous formation by directly binding to Penicillin Binding Protein 3 (PBP3) and inhibiting septal division after doubling of cells²⁵. Recent studies on *E. coli* showed that ampicillin treatment leads to filamentous PC formation with high reactive oxygen species (ROS)²⁶, while rifampicin treatment leads to rod-shaped and metabolically inactive²⁷ and ofloxacin treated persister were also elongated²⁸.

Stringent response (*relA* and *spoT*) is induced upon antibiotic exposure leading to increase in alarmone (p) ppGpp which arrests the cell growth (by directly interacting with RNA polymerase and inhibiting the transcription) and provides fitness advantage^{9,29}. Together with stringent response, the TA system activation also plays an important role in PC formation by reducing the cellular metabolism. In this study, enhanced expression of *relA*, *spoT* as well as *higA* and *higB* was observed, but the expression varied across the isolates (PAO1, TP-10, and ST-13) and changed with respect to antibiotic exposure (Fig. 4). A previous study has reported that *relA* gene was upregulated on treatment with colistin, amikacin, ciprofloxacin, and cefepime in the mid-exponential phase of *P. aeruginosa* clinical isolates¹⁰. Expression of *higA* and *higB* was also seen to be differentially responding upon exposure to different antibiotics amongst the isolates (Fig. 4). The elevated level of *higB* expression and its role in increasing the fraction of PCs was reported for ciprofloxacin¹⁰. TA affects the DNA gyrase activity, modulates the ribosome maturation, reduces the metabolism and growth to support the PC formation³¹. Upon gentamicin

treatment, the HigA antitoxin is degraded by Lon protease which enhances the expression of *higB* and *myfR*, and thus increases virulence gene expression^{12,30,32}. Our results show high expression of *relA*, *spoT* along with the *higA* and *higB* in the susceptible isolate (TP10) while *spoT* and *lon* in the resistant isolate (ST13). We hypothesize, PC formation occurred through activation of stringent response and TA system in susceptible isolate. Whereas in resistant isolate the PC formation is regulated by *spoT* and *lon*.

Another aspect of this study is to analyse the PC formation in biofilm with regard to antibiotic treatments. Biofilm is difficult to eradicate owing to its high tolerance towards antibiotics^{7,33}, and its transition towards persister phenotype in *P. aeruginosa* is not fully elucidated. These antibiotic-induced dormant cells are one of the reasons for biofilm tolerance³⁴ and the cause of recurrent biofilm-mediated infection. Studies on *P. aeruginosa* biofilm have been reported by using CLSM with Syto 9 (stains live cells) and PI (stains dead cells) dye where β -lactam treatment showed the filamentous formation of cells, disruption of biomass, and regrowth of biofilm^{35,36}. Further, aminoglycosides resulted in the decline of biofilm biomass, and the live cells were observed in the inner layer of biofilm³⁵. Tolerance towards aminoglycosides was reported due to oxygen limitation, low metabolic activity within the inner layers of biofilm, and slow diffusion of antibiotics through biomass^{37–39}. While fluoroquinolone treatment, particularly ciprofloxacin resulted in a deep decline in biofilm structure, dead cells, and disruption of biofilm biomass³⁹. Ciprofloxacin is associated with the formation of vacuoles, and cell lysis, which results in the extrusion of intracellular components⁴⁰. In the present study, firstly the thickness of biofilms formed by the three isolates varied and was different even between the strong biofilm forming isolates (PAO1 and ST13) (Fig. S1). The reason for this is due to the varying adhesion and twitching motility behaviour⁴¹. Also, when antibiotics with a different mode of action were used it showed unpredictability in the survival amongst the isolates. This is attributed to the varying degree of penetration of antibiotics due to the different biofilm thickness. Wide variation in PCs formation amongst isolates in response to different antibiotics was previously reported for other bacteria as well^{34,42,43}. This indicates that persistence not only depends upon the class of antibiotics but it also responds differently because of heterogeneity amongst the isolates and growth phase.

In the biofilm stage the expression of the stringent response, as well as toxin-antitoxin genes, was different across isolates. Ceftazidime treatment showed significant upregulation in stringent response as well as toxin-antitoxin genes followed by gentamicin (Fig. 8). Biofilms generated by a *P. aeruginosa* $\Delta relA spoT$ double knockout mutant were found to be more susceptible to fluoroquinolones, meropenem, colistin, and gentamicin²⁹. In the present data, in spite of increased *lon* expression the expression of *higA* was reduced and there was no change in expression of *higB* in PAO1 biofilm upon ceftazidime treatment (Fig. 8c–e). This indicates that transcriptional level of *higA* and *higB* are additionally regulated by unknown transcriptional regulator in biofilm stage and similar observation was reported by Song et al. 2020⁴⁴. Additionally, beta-lactam (ceftazidime) did not affect the persister level via Lon protease activation⁴⁵. Further, when *P. aeruginosa* biofilm is exposed to gentamicin, Lon protease is activated, which degrades the antitoxin HigA, and transcription of toxin *higB* was reported to increase^{12,30}. Guo et al. 2019 showed upregulation of *higB* gene after 30 min of exposure to gentamicin, due to degradation of HigA protein by Lon protease in late stationary phase cells³². Stringent response genes *relA*, *spoT* and *lon* as well as toxin-antitoxin gene *higBA* were elevated upon ciprofloxacin treatment when analysed after 1 h of exposure²⁰. Same study also reported stable gene expression in of stringent response after 4 h and no upregulation of *higB* gene. This significant difference in gene expression amongst the isolates suggests that biofilm persistence is highly strain-specific, depending upon the degree of biofilm formation, as well as the level of antibiotic exposure. This study provides the preliminary evidence on multiple dynamics of PC formation in clinical isolates. However, further complete transcriptomics studies will give better understanding of key molecular mechanism of PC formation.

This study shows that in the planktonic stage ceftazidime treatment gave rise to PCs to a greater extent than the other tested antibiotics, while on the other hand, in the biofilm stage gentamicin and ciprofloxacin gave rise to PCs. Taken together this study suggest that activation of stringent response and type II TA system differently contributed to the PC formation in response to different antibiotics.

Material and method

Bacterial strains, growth conditions, and antibiotics used for the study. In this study, UTIs causing *P. aeruginosa* isolates (TP-10 and ST-13) and PAO1 strain were used. Bacterial isolates were routinely sub-cultured on Pseudomonas Isolation Agar (PIA). Minimum Inhibitory Concentration (MIC) was determined in Muller Hinton Broth (MHB). Three antibiotics: ceftazidime (cell wall inhibitor), Gentamicin (protein inhibitor), and Ciprofloxacin (DNA gyrase inhibitor) were used for this study.

Minimum inhibitory concentration (MIC) determination. In the 96-well microtiter plate, the MIC was determined according to the CLSI guideline⁴⁶. Briefly, 100 μ l of Mueller Hinton Broth (MHB) was dispensed into the microtiter plate, followed by 50 μ l of 4 \times desired antibiotic (dissolved in MHB) concentration was added to each well. Thereafter, 50 μ l of 1:100 diluted culture (0.08 OD at 600 nm) was added to each well and incubated at 37 °C for 24 h under static conditions. Additionally, a growth control was grown without antibiotics. The MIC was concluded at the lowest concentration of three antibiotics that inhibited visible growth. The experiment was performed in biological triplicate for each strain.

Planktonic persister assay. Cell viability count was measured after antibiotic treatment to determine the presence of PC formation. The PCs formation was determined for PAO1, TP-10, and ST-13 as reported previously⁴⁷. To determine PCs formation in the planktonic stage, 3 ml of 0.1 OD at 600 nm culture was treated with 5 \times MIC concentration of antibiotics (ceftazidime, gentamicin, and ciprofloxacin) and kept on agitation at 250 rpm for 24 h in Luria Bertini (LB) medium. Colony-forming units (c.f.u.) were determined at time points of

t = 0 h, 2 h, 4 h, 6 h, 8 h, and 24 h by sampling one strain per tube. Briefly, 100 μ l of culture was sampled; washed with Phosphate Buffer Saline (PBS); serially diluted followed by spreading on Luria Agar (LA) plate, and incubated at 37 °C for 24 h for c.f.u. determination. The experiment was performed in biological triplicates.

Cellular redox activity in the planktonic stage. The cellular redox activity was studied after 4 h of antibiotic treatment at 5 \times MIC using RSG (Redox Sensor Green) and PI (Propidium iodide) staining. Briefly, the overnight grown culture was diluted to 0.1 OD at 600 nm in 3 ml LB and treated with antibiotic treatments as per the above-mentioned protocol. After 4 h of antibiotic treatment, 3 ml of sample was aliquoted, washed with PBS twice, and resuspended in 300 μ l of PBS. For flow cytometry, the cells were stained using RSG (1 μ l) and PI (1 μ l of 1:100 diluted) dyes (BacLight™ RedoxSensor™ Green Vitality Kit Thermo Fisher Scientific Inc., Waltham, MA, USA) for 10 min in dark condition. No antibiotic treatment was used as a control. The flow cytometry (Becton Dickinson FACS Calibur, New Jersey, United States) was performed for the detection of fluorescence signals using FL1 and FL3 channels. The RSG-positive cells were plotted in a histogram against the FL1 channel. The data were analysed using three independent biological triplicates²⁷.

Fluorescence microscopy. PCs formation was observed after 4 h of antibiotic treatment according to the procedure outlined above. After 4 h of incubation, 1 ml of sample was aliquoted; PBS wash was given to remove any residual antibiotic. The sample was resuspended in 100 μ l of PBS and stained with 1 μ l RSG and 1 μ l of 1:100 diluted PI concentration. Thereafter, 10 μ l of the sample was spotted on a 1% agarose pad and covered with a 22 mm coverslip. The cells were viewed under a 100X oil immersion fluorescence (BX 51 Olympus microscope, Japan) microscope. For dead cells, cells were treated with ethanol and as a control, no antibiotic treatment was used²⁷. The experiment was performed in triplicates.

Gene expression in the planktonic stage. After 4 h of antibiotic treatment with 5X MIC, 3 ml of cells were centrifuged for 5 min at 8000 rpm and cells were washed in PBS to remove antibiotics and resuspended in 300 μ l PBS. Total RNA was extracted using the Nucleospin RNA kit (Macherey Nagel, Hoerd, France) and DNase treatment was performed as per the manufacturer's instruction. On a 2% gel, RNA integrity was verified and quantified using nanodrop (Thermo Fisher Scientific, Waltham, MA, USA). The First-strand cDNA synthesis was performed with a prime 1st Strand cDNA synthesis kit (Takara, Bio in, Japan) per protocol. The stringent response genes (*relA*, *spoT*, and *lon*), as well as toxin-antitoxin genes (*higA* and *higB*), were studied using the primer listed in Supplementary Table S2. The PCR cycling conditions were as follows: 95 °C for 5 min and 40 cycles of 95 °C for 30 s, 58 °C for 30 s, 72 °C for 30 s. Relative quantification was carried out from three independent biological replicates. Data were normalized to untreated and fold changes were calculated according to the $2^{-\Delta\Delta Ct}$ method⁴⁸.

Biofilm model. In the six well polystyrene plates, 3 ml of bacterial culture (0.01 OD at 600 nm) was added and incubated at 37 °C for 24 h in static conditions. The next day, planktonic suspensions were removed and biofilms were gently rinsed with 1 ml of 0.85% NaCl to remove planktonic cells. Thereafter, 3 ml of fresh MHB was added and challenged with a 5 \times MIC concentration of antibiotics for 24 h²⁰.

Biofilm quantification. According to Stepanovic et al. 2004, the biofilm was grown in the 96-well plates. Briefly, 20 μ l of overnight culture (0.2 OD at 600 nm) and 230 μ l of LB were kept at 37 °C for 24 h of incubation. Only LB was used as blank control. The next day, biofilm was rinsed with 0.85% saline; fixed with methanol for 15 min; stained with 0.1% crystal violet (CV) for 15 min; CV was removed and rinsed with distilled water (DW) twice; air-dried and a further 33% glacial acetic was used to dissolve the attached CV. According to Stepanović et al. 2004, biofilm formation was quantified at 570 nm and categorized into strong, moderate, and weak based on cut-off OD (ODc) value (three standard deviations above the mean OD of the negative control)⁴⁹. Isolates were categorized as: no biofilm producer (OD \leq ODc), weak biofilm producers (ODc < OD < 2 \times ODc), moderate biofilm producers (2 \times ODc < OD < 4 \times ODc), and strong biofilm producers (4 \times ODc < OD). The experiment was performed in three biological replicates.

Biofilm persister assay. In this study, the biofilm was formed as mentioned above for 24 h and treated with different antibiotics (ceftazidime, gentamicin, and ciprofloxacin) with 5 \times MIC for another 24 h and untreated was used as control. Cell viability was measured at t = 0 h, 2 h, 4 h, 6 h, 8 h, and 24 h for each antibiotic treatment according to Soares et al. 2019²⁰. All experiments were performed in triplicates.

Cellular redox activity in the biofilm stage. The Biofilm was formed for 24 h and treated with antibiotics as per above mention protocol. After 4 h of antibiotic treatments, the biofilm was once rinsed with 1 ml of 0.85% NaCl to remove planktonic cells and antibiotic. The biofilm was resuspended in 300 μ l of 0.85% NaCl and stained with RSG (1 μ l) and PI (1 μ l of 1:100 diluted) dyes and incubated for 10 min in dark conditions. The untreated biofilm was used as a control. For flow cytometry, the instrument and settings were the same as per above mention protocol.

Confocal laser scanning microscopy (CLSM) of biofilm. The PCs formation was studied in the biofilm using CLSM. After 5 \times MIC of antibiotic treatment for 4 h, biofilm was rinsed with 1 ml of 0.85% NaCl to remove planktonic cells and antibiotic. Further, the biofilm was stained with an RSG (1 μ l) and PI (1 μ l 1:100 diluted)

dyes. To remove excess stain from the biofilm a gentle wash with 1 ml of 0.85% NaCl was given. The untreated biofilm was used as a control. The biofilm visualization was done using Carl Zeiss CLSM 780 microscope.

Gene expression in the biofilm stage. RNA was extracted from the biofilm grown after 4 h of antibiotic treatment. After 4 h of antibiotic treatment with 5X MIC, biofilm was rinsed once with 1 ml of 0.85% NaCl. The remaining biofilm was then pooled in 1 ml of 0.85% NaCl, centrifuged at 8000 rpm for 5 min, and resuspended in 1 ml of 0.85% NaCl. The untreated biofilm was used as a control. The cDNA synthesis and qRT-PCR were performed using the primer listed in Supplementary Table S2 as per above mention protocol for planktonic gene expression.

Statistical analysis. All experiments were carried out in three biological triplicates. The statistical analysis was carried out using the One-way and Two-way ANOVA test through Graph Prism 9.

Data availability

All data generated or analysed during this study are included in this published article [and its supplementary information files].

Received: 6 July 2022; Accepted: 9 September 2022

Published online: 27 September 2022

References

1. Kwan, B. W., Valenta, J. A., Benedik, M. J. & Wood, T. K. Arrested protein synthesis increases persister-like cell formation. *Antimicrob. Agents Chemother.* **57**, 1468–1473 (2013).
2. Hobby, L., Karl, M. & Eleanor, C. Observations on the mechanism of action of penicillin. *Proc. Soc. Exp. Biol. Med.* **50**, 281–285 (1942).
3. Bigger, J. W. Treatment of Staphylococcal infections with penicillin by intermittent sterilisation. *Lancet* **244**, 497–500 (1944).
4. Lewis, K. Multidrug tolerance of biofilms and persister cells. *Curr. Top. Microbiol. Immunol.* **322**, 107–131 (2008).
5. Fauvarot, M., de Groot, V. N. & Michiels, J. Role of persister cells in chronic infections: Clinical relevance and perspectives on anti-persister therapies. *J. Med. Microbiol.* **60**, 699–709 (2011).
6. Percival, S. L., Hill, K. E., Malic, S., Thomas, D. W. & Williams, D. W. Antimicrobial tolerance and the significance of persister cells in recalcitrant chronic wound biofilms. *Wound Repair Regen.* **19**, 1–9 (2011).
7. Costerton, J. W., Stewart, P. S. & Greenberg, E. P. Bacterial biofilms: A common cause of persistent infections. *Science* **284**, 1318–1322 (1999).
8. Ciofu, O., Tolker-Nielsen, T., Jensen, P. Ø., Wang, H. & Hoiby, N. Antimicrobial resistance, respiratory tract infections and role of biofilms in lung infections in cystic fibrosis patients. *Adv. Drug Deliv. Rev.* **85**, 7–23 (2015).
9. Moradali, M. F., Ghods, S. & Rehm, B. H. A. *Pseudomonas aeruginosa* lifestyle: A paradigm for adaptation, survival, and persistence. *Front. Cell. Infect. Microbiol.* **7**, 644 (2017).
10. Baek, M. S., Chung, E. S., Jung, D. S. & Ko, K. S. Effect of colistin-based antibiotic combinations on the eradication of persister cells in *Pseudomonas aeruginosa*. *J. Antimicrob. Chemother.* **75**, 917–924 (2020).
11. Harms, A., Maisonneuve, E. & Gerdes, K. Mechanisms of bacterial persistence during stress and antibiotic exposure. *Science* **354**, 4268 (2016).
12. Marr, A. K., Overhage, J., Bains, M. & Hancock, R. E. W. The Lon protease of *Pseudomonas aeruginosa* is induced by aminoglycosides and is involved in biofilm formation and motility. *Microbiology* **153**, 474–482 (2007).
13. Soares, A., Alexandre, K. & Etienne, M. Tolerance and persistence of *Pseudomonas aeruginosa* in biofilms exposed to antibiotics: Molecular mechanisms, antibiotic strategies and therapeutic perspectives. *Front. Microbiol.* **11**, 1–11 (2020).
14. Viducic, D. *et al.* Functional analysis of *spoT*, *relA* and *dksA* genes on quinolone tolerance in *Pseudomonas aeruginosa* under nongrowing condition. *Microbiol. Immunol.* **50**, 349–357 (2006).
15. Muthuramalingam, M., White, J. C., Murphy, T., Ames, J. R. & Bourne, C. R. The toxin from a ParDE toxin-antitoxin system found in *Pseudomonas aeruginosa* offers protection to cells challenged with anti-gyrase antibiotics. *Mol. Microbiol.* **111**, 441–454 (2019).
16. Li, G. *et al.* Identification and characterization of the HicAB toxin-antitoxin system in the opportunistic pathogen *Pseudomonas aeruginosa*. *Toxins (Basel)* **8**, 1–12 (2016).
17. Coskun, U. S. *et al.* Effect of MazEF, HigBA and RelBE toxin-antitoxin systems on antibiotic resistance in *Pseudomonas aeruginosa* and *Staphylococcus* isolates. *Malawi Med. J.* **30**, 67–72 (2018).
18. Wood, T. L. & Wood, T. K. The HigB/HigA toxin/antitoxin system of *Pseudomonas aeruginosa* influences the virulence factors pyochelin, pyocyanin, and biofilm formation. *Microbiologyopen* **5**, 499–511 (2016).
19. Zhang, Y. *et al.* HigB reciprocally controls biofilm formation and the expression of type III secretion system genes through influencing the intracellular c-di-GMP level in *Pseudomonas aeruginosa*. *Toxins (Basel)* **10**, 1–12 (2018).
20. Soares, A., Roussel, V., Pestel-caron, M., Barreau, M. & Etienne, M. Understanding Ciprofloxacin failure in *Pseudomonas aeruginosa* biofilm: Persister cells survive matrix disruption. *Front. Microbiol.* **10**, 2603 (2019).
21. Orman, M. A., Henry, T. C., Decoste, C. J., Brynildsen, M. P. & Engineering, B. Analyzing persister physiology with fluorescence activated cell sorting. in *Bacterial Persistence*. Vol. 1333. 83–100. (Humana Press, 2016).
22. Orman, M. A. & Brynildsen, M. P. Dormancy is not necessary or sufficient for bacterial persistence. *Antimicrob. Agents Chemother.* **57**, 3230–3239 (2013).
23. Spoering, A. M. Y. L. & Lewis, K. I. M. Biofilms and planktonic cells of *Pseudomonas aeruginosa* have similar resistance to killing by antimicrobials. *J. Bacteriol.* **183**, 6746–6751 (2001).
24. Brooun, A., Liu, S. & Lewis, K. A dose-response study of antibiotic resistance in *Pseudomonas aeruginosa* biofilms. *Antimicrob. Agents Chemother.* **44**, 640–646 (2000).
25. Buijs, J., Dofferhoff, A. S. M., Mouton, J. W., Wagenvoort, J. H. T. & Van Der Meer, J. W. M. Concentration-dependency of β -lactam-induced filament formation in Gram-negative bacteria. *Clin. Microbiol. Infect.* **14**, 344–349 (2008).
26. Sulaiman, J. E. & Lam, H. Proteomic study of the survival and resuscitation mechanisms of filamentous persisters in an evolved *Escherichia coli* population from cyclic ampicillin treatment. *mSystems* **5**, 1–21 (2020).
27. Kim, J. S., Yamasaki, R., Song, S., Zhang, W. & Wood, T. K. Single cell observations show persister cells wake based on ribosome content. *Environ. Microbiol.* **20**, 2085–2098 (2018).
28. Völzing, K. G. & Brynildsen, M. P. Stationary-phase persisters to ofloxacin sustain DNA damage and require repair systems only during recovery. *MBio* **6**, 1–11 (2015).

29. Nguyen, D. *et al.* Active starvation responses mediate antibiotic tolerance in biofilms and nutrient-limited bacteria. *Science* **334**, 982–986 (2011).
30. Li, M. *et al.* HigB of *Pseudomonas aeruginosa* enhances killing of phagocytes by up-regulating the type III secretion system in ciprofloxacin induced persister cells. *Front. Cell. Infect. Microbiol.* **6**, 1–14 (2016).
31. Page, R. & Peti, W. Toxin-antitoxin systems in bacterial growth arrest and persistence. *Nat. Chem. Biol.* **12**, 208–214 (2016).
32. Guo, Y. *et al.* Antitoxin HigA inhibits virulence gene mvfR expression in *Pseudomonas aeruginosa*. *Environ. Microbiol.* **21**, 2707–2723 (2019).
33. Donlan, R. M. Biofilm formation: A clinically relevant microbiological process. *Clin. Infect. Dis.* **33**, 1387–1392 (2001).
34. Amato, S. M. & Brynildsen, M. P. Nutrient transitions are a source of persisters in *Escherichia coli* biofilms. *PLoS ONE* **9**, 93110 (2014).
35. Rojo-Moliner, E. *et al.* Sequential treatment of biofilms with aztreonam and tobramycin is a novel strategy for combating *Pseudomonas aeruginosa* chronic respiratory infections. *Antimicrob. Agents Chemother.* **60**, 2912–2922 (2016).
36. Gómez-junyent, J. *et al.* Efficacy of ceftolozane/tazobactam, alone and in combination with colistin, against multidrug-resistant *Pseudomonas aeruginosa* in an in vitro biofilm pharmacodynamic model. *Int. J. Antimicrob. Agents* **53**, 612–619 (2019).
37. Borriello, G. *et al.* Oxygen limitation contributes to antibiotic tolerance of *Pseudomonas aeruginosa* in biofilms. *Antimicrob. Agents Chemother.* **48**, 2659–2664 (2004).
38. Walters, M. C. III, Roe, F., Bugnicourt, A., Franklin, M. J. & Stewart, P. S. Contributions of antibiotic penetration, oxygen limitation, and low metabolic activity to tolerance of *Pseudomonas aeruginosa* biofilms to ciprofloxacin and tobramycin. *Antimicrob. Agents Chemother.* **47**, 317–323 (2003).
39. Hatch, R. A. & Schiller, N. L. Alginate lyase promotes diffusion of aminoglycosides through the extracellular polysaccharide of mucoid *Pseudomonas aeruginosa*. *Antimicrob. Agents Chemother.* **42**, 974–977 (1998).
40. Elliott, T. S. J., Shelton, A. & Greenwood, D. The response of *Escherichia coli* to ciprofloxacin and norfloxacin. *J. Med. Microbiol.* **23**, 83–88 (1987).
41. Patel, H. & Gajjar, D. Cell adhesion and twitching motility influence strong biofilm formation in *Pseudomonas aeruginosa*. *Biofouling* **38**, 235–249 (2022).
42. Gallo, S. W., Donamore, B. K., Pagnussatti, V. E., Ferreira, C. A. S. & De Oliveira, S. D. Effects of meropenem exposure in persister cells of *Acinetobacter calcoaceticus-baumannii*. *Future Microbiol.* **12**, 131–140 (2017).
43. Drescher, S. P. M., Gallo, S. W., Ferreira, P. M. A., Ferreira, C. A. S. & de Oliveira, S. D. Salmonella enterica persister cells form unstable small colony variants after in vitro exposure to ciprofloxacin. *Sci. Rep.* **9**, 1–11 (2019).
44. Song, Y. *et al.* *Pseudomonas aeruginosa* antitoxin HigA functions as a diverse regulatory factor by recognizing specific pseudo-palindromic DNA motifs. *Environ. Microbiol.* **23**, 1541–1558 (2021).
45. Chowdhury, N., Kwan, B. W. & Wood, T. K. Persistence increases in the absence of the alarmone guanosine tetraphosphate by reducing cell growth. *Sci. Rep.* **6**, 1–9 (2016).
46. Wiegand, I., Hilpert, K. & Hancock, R. E. W. Agar and broth dilution methods to determine the minimal inhibitory concentration (MIC) of antimicrobial substances. *Nat. Protoc.* **3**, 163–175 (2008).
47. Mulcahy, L. R., Burns, J. L., Lory, S. & Lewis, K. Emergence of *Pseudomonas aeruginosa* strains producing high levels of persister cells in patients with cystic fibrosis. *J. Bacteriol.* **192**, 6191–6199 (2010).
48. Guyard-Nicodème, M. *et al.* Outer membrane modifications of *Pseudomonas fluorescens* MF37 in response to hyperosmolarity. *J. Proteome Res.* **7**, 1218–1225 (2008).
49. Stepanović, S., Cirković, I., Ranin, L. & Švabić-Vlahović, M. Biofilm formation by *Salmonella* spp. and *Listeria monocytogenes* on plastic surface. *Lett. Appl. Microbiol.* **38**, 428–432 (2004).

Acknowledgements

We would like to acknowledge “Confocal Laser Scanning Microscopy (Carl Zeiss LSM 710) housed in Central Facility at VSI-CMB Department of MSU Baroda”. We would also like to acknowledge Dr. Ratika Srivastava and Khushboo Rana for helping in flow cytometry experiments.

Author contributions

D.G. and H.P. designed the experiments. H.P. carried out the experiments. H.P., D.G., and H.B. analysed the data and wrote the manuscript.

Funding

This work was supported by research grant from ICMR (Project number: 5/4/3/2012-RMC). Hiral Patel thanks CSIR-UGC fellowship-University Grants Commission (UGC). We are also thankful for the infrastructure support to this department under the DST-FIST program of Government of India and Biotechnology Teaching programme.

Competing interests

The authors declare no competing interests.

Additional information

Supplementary Information The online version contains supplementary material available at <https://doi.org/10.1038/s41598-022-20323-3>.

Correspondence and requests for materials should be addressed to D.G.

Reprints and permissions information is available at www.nature.com/reprints.

Publisher's note Springer Nature remains neutral with regard to jurisdictional claims in published maps and institutional affiliations.

www.nature.com/scientificreports/



Open Access This article is licensed under a Creative Commons Attribution 4.0 International License, which permits use, sharing, adaptation, distribution and reproduction in any medium or format, as long as you give appropriate credit to the original author(s) and the source, provide a link to the Creative Commons licence, and indicate if changes were made. The images or other third party material in this article are included in the article's Creative Commons licence, unless indicated otherwise in a credit line to the material. If material is not included in the article's Creative Commons licence and your intended use is not permitted by statutory regulation or exceeds the permitted use, you will need to obtain permission directly from the copyright holder. To view a copy of this licence, visit <http://creativecommons.org/licenses/by/4.0/>.

© The Author(s) 2022